RUB-TPII-25/95

# Sphaleron transitions in the Minimal Standard Model and the upper bound for the Higgs Mass

**Dmitri Diakonov*[1], Maxim Polyakov*, Peter Sieber◇, Jörg Schaldach◇, and Klaus Goeke◇[2]**

*Petersburg Nuclear Physics Institute, Gatchina, St. Petersburg 188350, Russia

◇Institut für Theor. Physik II, Ruhr-Universität Bochum, D-44780 Bochum, Germany

**Abstract**

We calculate the dissipation of the baryon number after the electroweak phase transition due to thermal fluctuations above the sphaleron barrier. We consider not only the classical Boltzmann factor but also fermionic and bosonic one-loop contributions. We find that both bosonic and especially fermionic fluctuations can considerably suppress the transition rate. Assuming the Langer–Affleck formalism for this rate, the condition that an initial baryon asymmetry must not be washed out by sphaleron transitions leads, in the Minimal Standard Model ($\sin\theta_W = 0$), to an upper bound for the Higgs mass in the range 60 to 75 GeV.

[1] diakonov@lnpi.spb.su

[2] goeke@hadron.tp2.ruhr-uni-bochum.de

# 1 Introduction

The question about the origin of the baryon asymmetry of the Universe (BAU) has recently gained much interest. Many different models of how the BAU was created are being discussed in the literature (for reviews see e.g. [1]), some of them considering BAU generation at the GUT stage of the Universe, others favoring the generation during the electroweak phase transition.

Whatever the mechanism was which led to the BAU at early times, the resulting asymmetry might have been eliminated by baryon number violating processes in the electroweak theory after the phase transition. Such processes are possible due to the anomaly of baryon and lepton currents [2] and the non-trivial topological structure of the Yang–Mills theory. This feature was discovered in 1976 by Faddeev [3] and Jackiw and Rebbi [4], who found that the potential energy is periodic in a certain functional of the fields, the Chern–Simons number $N_{\rm CS}$. Topologically distinct vacua of the theory are enumerated by integer $N_{\rm CS}$. In the electroweak theory those vacua are separated by an energy barrier whose height is of the order of $m_W/\alpha$ where $m_W$ is the mass of the $W$ boson and $\alpha = g^2/(4\pi)$ is the $SU(2)$ gauge coupling constant.

Transitions from one vacuum to a topologically distinct one over this barrier change the baryon and lepton number by one unit per fermion generation due to the anomaly of the corresponding currents. If we assume in accordance with the standard model that $B - L$ (baryon minus lepton number) is conserved and that there is no primordial excess of say, antileptons, then these transitions can cause the BAU erasure as mentioned above. Hence it is necessary to know the transition rate of such processes. While the baryon number of the Universe today ($B_0$) is about $10^{-9}$ to $10^{-10}$ (relative to the number of relict photons), in models generating the BAU at the electroweak phase transition the number of produced baryons ($B_{T_c}$) per photon is of order $10^{-5}$ [5, 6]. (The precise value is not important for our calculation, see below). Thus the ratio $B_0/B_{T_c}$ which describes the dissipation of the BAU should not be significantly lower than about $10^{-5}$, otherwise the initial baryon excess is not large enough to explain the present day BAU.

In principle to obtain the value of this ratio one has to integrate the rate of the baryon number violating processes over the temperature from $T = T_c$ to $T = 0$. In practice, however, the rate is very strongly suppressed at ordinary temperatures [2] so that only a short range below $T_c$ contributes to the erasure of the BAU. While

at low $T$ the rate is dominated by tunnelling processes, at higher temperatures the energy barrier can be overcome thanks to thermal fluctuations [7, 8, 5]. This thermal transition rate can be evaluated by the semi-classical formalism of Langer [9] and Affleck [10].

A key role in this calculation is played by the static classical field configuration which corresponds to the top of the energy barrier, having Chern–Simons number $N_{\rm CS} = \frac{1}{2}$. This configuration was first found by Dashen, Hasslacher and Neveu [11] and rediscovered in the context of electroweak theory by Klinkhamer and Manton, it is called sphaleron [12]. Its energy $E_{\rm class}$ enters the transition rate $\gamma(T) = A(T)\, e^{-E_{\rm class}/T}$ via the classical Boltzmann factor and is usually the dominant contribution to $\gamma$, i.e. in most cases $|\ln A(T)| < E_{\rm class}/T$. The prefactor $A(T)$ contains contributions coming from fermion and boson quantum fluctuations about the sphaleron. In [8] the rate was calculated considering the classical and zero-mode contributions, while the determinant of non-zero boson fluctuation modes and the fermion determinant were set to unity. The result for $\gamma$ was so large that any initial baryon excess would have been washed out by sphaleron transitions after the phase transition. Therefore it is of interest whether quantum loop corrections could help to preserve the baryon asymmetry.

Several investigations which consider loop corrections have already been made. Bochkarev and Shaposhnikov [5, 6] included the boson fluctuations through an effective potential of the Higgs field. They obtained that the transition rate is sufficiently suppressed if the Higgs mass is below an upper limit of 45 to 55 GeV. A direct computation of the bosonic determinant over non-zero modes was made in [13] by using an approximation technique [14], exact calculations were performed in [15, 16].

All these calculations were based on the high temperature limit in which the four-dimensional fluctuation matrix can be replaced by the three-dimensional one and fermions decouple completely. Although parametrically this limit is reasonable it need not necessarily be justified numerically. In this paper we go beyond the high temperature approximation which corresponds to taking into account the fermion determinant (suppressed in the formal high temperature limit) and to calculating the full four-dimensional bosonic determinant. We generalize the preceeding calculations to arbitrary temperatures. First, we include fermion loops which previously have been altogether neglected, second, we evaluate the fluctuation determinants for finite temperature considering the full sum over Matsubara frequencies. Both contributions

seem to be quite essential numerically.

The fermion determinant has been considered in detail in our previous publication [17], the bosonic one is the aim of this work (see also [18]). We find that the result is significantly influenced by terms which vanish in the formal high $T$ limit, especially by the contribution of the fermion fluctuations. Actually, the polarization of the Dirac sea of fermions in the classical sphaleron background field adds up to about 30 % to the sphaleron energy. Therefore, the fermion determinant which was put to unity in [5, 8, 13, 15, 16] leads to a strong additional suppression of the transition rate.

Let us remark that in an abelian (1+1)-dimensional model the transition rate can be calculated analytically. This has been done in [19] for the boson and in [20] for the fermion loop correction. In (3+1) dimensions, however, one has to resort to numerical methods.

For the evaluation of the boson determinant we use the same method as for the fermion determinant in [17]. It is based on the computation of the complete (discretized) spectrum of the fluctuation operators. All the relevant quantities can subsequently be calculated for any temperature $T$ by suitable summations over the eigen-energies. Including the loop corrections into the formula for the transition rate, we finally obtain the ratio $B_0/B_{T_c}$ which is a measure for the erasure of the BAU. We find that both bosonic and fermionic fluctuations suppress the rate considerably, especially for a low mass of the Higgs boson and a large top quark mass. For a top quark mass in the range $m_t = 150$ to 200 GeV, in accordance to recent experimental results [21], the condition that the BAU must not be washed out by sphaleron transitions leads within the framework of our one-loop calculation and the Langer–Affleck formalism to an upper limit for $m_H$ in the range between about 60 and 75 GeV.

Another goal of this work is the recalculation of the boson fluctuation determinant in the high $T$ limit since the results of the two existing calculations [15, 16], based on different analytical and numerical techniques, deviate from each other. Although they show the same tendency for low Higgs masses, no satisfactory quantitative agreement was found. Our numerical method is based on the diagonalization of the fluctuation operator as described above; it differs significantly from those used in [15, 16] so that our study can be considered as independent. We find that our results for the boson determinant in the high $T$ limit agree with the results of [16] up to about 10% while there is a larger deviation from the ones of [15].

The paper is organized as follows: In Section 2 we introduce into the notations

and conventions of the model, in Section 3 we apply the Langer–Affleck formalism to the baryon number violation processes. The renormalization is discussed in Section 4, followed by the treatment of the temperature dependent parts of the fluctuations. The evaluation of the baryon erasure $B_0/B_{T_c}$ is done in Section 6. Numerical results and checks for the computation of the fluctuation determinants are presented in Section 7. In Section 8 we proceed to the evaluation of the sphaleron transition rate and deduce the upper bound for the Higgs mass. We also investigate the applicability of the framework of our calculation. Finally we summarize the results and draw our conclusions in Section 9. Technical details about the computation of the discretized spectrum and the spectral densities are treated in the appendices.

# 2 The model and parameters

We consider the minimal version of the standard electroweak theory with one Higgs doublet which is Yukawa coupled to left handed fermion doublets and to right handed singlets; in the following we write only one doublet and one pair of singlets for brevity.

We shall work in the limit of the vanishing Weinberg angle, i.e. the theory is reduced to the pure $SU(2)$ case (without the $U(1)$). This idealization does not seem to be significant [22]. The Lagrangian is thus

$$\begin{aligned}\mathcal{L} &= -\frac{1}{4g^2}F^a_{\mu\nu}F^{a\,\mu\nu} + (D_\mu\Phi)^\dagger(D^\mu\Phi) - \frac{\lambda^2}{2}\Big(\Phi^\dagger\Phi - \frac{v^2}{2}\Big)^2 \\ &\quad + \bar\psi_L i\gamma^\mu D_\mu\psi_L + \bar\psi_R i\gamma^\mu\partial_\mu\psi_R - \bar\psi_L M\psi_R - \bar\psi_R M^\dagger\psi_L \end{aligned} \tag{2.1}$$

with the covariant derivative $D_\mu = \partial_\mu - iA_\mu$ , $A_\mu = \frac{1}{2}A^a_\mu\tau^a$, and the field strength $F_{\mu\nu} = \frac{1}{2}F^a_{\mu\nu}\tau^a = i[D_\mu, D_\nu]$ , $F^a_{\mu\nu} = \partial_\mu A^a_\nu - \partial_\nu A^a_\mu + \epsilon^{abc}A^b_\mu A^c_\nu$. $M$ is a $2\times 2$ matrix built of the Higgs field components $\Phi = \binom{\Phi^+}{\Phi^0}$ and the Yukawa couplings $h_u, h_d$:

$$M = \begin{pmatrix} h_u\Phi^{0*} & h_d\Phi^+ \\ -h_u\Phi^{+*} & h_d\Phi^0 \end{pmatrix}. \tag{2.2}$$

$\psi_L$ means the $SU(2)$ fermion doublet

$$\psi_L = \tfrac{1}{2}(1-\gamma_5)\psi = \begin{pmatrix}\psi^u_L \\ \psi^d_L\end{pmatrix} \tag{2.3}$$

and with $\psi_R$ we denote the pair of the singlets

$$\psi_R = \tfrac{1}{2}(1+\gamma_5)\psi = \begin{pmatrix}\psi^u_R \\ \psi^d_R\end{pmatrix}. \tag{2.4}$$

The masses generated by the non-vanishing vacuum expectation value $\langle 0|\Phi|0\rangle = \frac{v}{\sqrt{2}}\binom{0}{1}$ are

$$m_W = \frac{gv}{2}\,, \qquad m_{u,d} = \frac{h_{u,d}v}{\sqrt{2}}\,, \qquad \text{and} \qquad m_H = \lambda v \tag{2.5}$$

for the gauge boson, the fermions, and the Higgs boson.

We prefer to work in terms of dimesionless rescaled quantities

$$x^\mu \to m_W^{-1} x^\mu\,, \qquad A^a_\mu \to m_W A^a_\mu\,, \qquad \Phi \to \frac{m_W}{\sqrt{2}\,g}\Phi\,; \tag{2.6}$$

using the following representation of the Dirac matrices

$$\gamma^0 = \begin{pmatrix} 0 & 1 \\ 1 & 0 \end{pmatrix}\,, \qquad \gamma^i = \begin{pmatrix} 0 & \sigma_i \\ -\sigma_i & 0 \end{pmatrix}\,, \qquad \gamma^5 = \begin{pmatrix} -1 & 0 \\ 0 & 1 \end{pmatrix}\,, \tag{2.7}$$

the fermion Dirac spinors can be reduced to two components:

$$\psi_L \to m_W^{3/2}\binom{\psi_L}{0}\,, \qquad \psi_R \to m_W^{3/2}\binom{0}{\psi_R}\,. \tag{2.8}$$

In this representation the Lagrangian (2.1) is

$$\begin{aligned} \mathcal{L} \;=\; & m_W^4\Big[\frac{1}{g^2}\Big(-\tfrac{1}{4}F^a_{\mu\nu}F^{a\,\mu\nu} + \tfrac{1}{2}(D_\mu\Phi)^\dagger(D^\mu\Phi) - \tfrac{1}{32}\nu_H^2(\Phi^\dagger\Phi - 4)^2\Big) \\ & + i\psi_L^\dagger(D_0 - \sigma_i D_i)\psi_L + i\psi_R^\dagger(\partial_0 + \sigma_i\partial_i)\psi_R - \psi_L^\dagger M\psi_R - \psi_R^\dagger M^\dagger\psi_L\Big]\,, \end{aligned} \tag{2.9}$$

with the mass matrix

$$M = \frac{1}{2m_W}\begin{pmatrix} m_u\Phi^{0*} & m_d\Phi^+ \\ -m_u\Phi^{+*} & m_d\Phi^0 \end{pmatrix} \qquad \text{and} \qquad \nu_{_H} = \frac{m_H}{m_W}\,. \tag{2.10}$$

# 3 The baryon number violation rate

As it is well known [2] the baryon and lepton numbers $B$ and $L$ are not conserved in the standard model of electroweak interactions due to the anomaly of the corresponding currents $j^\mu_B$ and $j^\mu_L$:

$$\partial_\mu j^\mu_B = \partial_\mu j^\mu_L = \frac{N_g}{64\pi^2}\epsilon^{\mu\nu\rho\sigma}F^a_{\mu\nu}F^a_{\rho\sigma}. \tag{3.1}$$

Here $N_g = 3$ is the number of fermion generations. We dropped the contribution of the $U(1)$ gauge field to the anomaly since we work in the approximation of vanishing Weinberg angle $\sin\theta_W = 0$.

Integrating this anomaly equation one finds that in any process the change of the baryon and lepton numbers is related to the change of the Chern–Simons number by

$$\Delta B = \Delta L = N_g \, \Delta N_{\rm CS} \; , \tag{3.2}$$

where the Chern–Simons number $N_{\rm CS}$ is defined by

$$N_{\rm CS} = \int d^3\mathbf{r} \, K_0(\mathbf{r}) \, , \tag{3.3}$$

$$K^\mu = \frac{1}{16\pi^2} \, \epsilon^{\mu\nu\rho\sigma} \left( A^a_\nu \partial_\rho A^a_\sigma + \tfrac{1}{3} \epsilon_{abc} A^a_\nu A^b_\rho A^c_\sigma \right) , \tag{3.4}$$

$$\partial_\mu K^\mu = \frac{1}{64\pi^2} \epsilon^{\mu\nu\rho\sigma} F^a_{\mu\nu} F^a_{\rho\sigma} \; . \tag{3.5}$$

The semiclassical description of the processes with fermion and lepton number violation is based on the existence of an infinite number of classical vacuum configurations labeled by integer values of $N_{\rm CS}$. These vacua are separated by potential barriers which can be overcome either by quantum tunnelling or by real processes in the Minkowskian time due to thermal fluctuations. We shall be interested in temperatures at which the real-time transitions dominate. The rate of the thermal transitions at temperature $T$ between adjacent vacua is roughly given by the Boltzmann factor $\exp(-E_{\rm class}/T)$, where $E_{\rm class}$ is the energy of the sphaleron, which is the field configuration at the top of the barrier between the two vacua. The transition rate $\Gamma$ with the preexponential factor is given by the Langer–Affleck formula [9, 10]

$$\Gamma = \frac{|\omega_-|}{\pi} \, \frac{{\rm Im} \, Z_{\rm sphal}}{Z_0} \; . \tag{3.6}$$

Here $Z_0$ is the partition function computed in the semiclassical approximation around the vacuum, and $Z_{\rm sphal}$ is the partition function obtained by semiclassical expansion about the sphaleron solution. Since the sphaleron solution is a saddle-like point of the potential energy functional, the quadratic form of fluctuations about the sphaleron has a negative mode $\omega_-^2 < 0$ so that the formal semiclassical expansion about the nonstable static solution gives a complex contribution to the partition function $Z_{\rm sphal}$.

In the Weinberg–Salam model the sphaleron solution in the temporal gauge $A_0 = 0$ can be found as a stationary point of the energy functional

$$E_{\rm class} = \frac{m_W}{g^2} \int d^3\mathbf{r} \, \left[ \tfrac{1}{4} (F^a_{ij})^2 + \tfrac{1}{2} (D_i \Phi)^\dagger (D_i \Phi) + \tfrac{1}{32} \nu_H^2 (\Phi^\dagger \Phi - 4)^2 \right] \; . \tag{3.7}$$

which leads to the classical equations

$$\begin{aligned}
&(D_i F_{ij})^a - \tfrac{i}{4}\Big(\Phi^\dagger \tau^a (D_j\Phi) - (D_j\Phi)^\dagger \tau^a \Phi\Big) = 0 \\
&\Big(D_i^2 - \tfrac{1}{8}\nu_H^2(\Phi^\dagger\Phi - 4)\Big)\Phi = 0\,.
\end{aligned} \tag{3.8}$$

The sphaleron solution is assumed to have the following form (hedgehog)

$$\begin{aligned}
\bar{A}_i^a(\mathbf{r}) &= \epsilon_{aij} n_j \,\frac{1-A(r)}{r} + (\delta_{ai} - n_a n_i)\,\frac{B(r)}{r} + n_a n_i\,\frac{C(r)}{r}\,, \\
\bar{\Phi}(\mathbf{r}) &= 2\Big[H(r) + iG(r)\,\mathbf{n}\cdot\boldsymbol{\varnothing}\Big]\binom{0}{1}\,.
\end{aligned} \tag{3.9}$$

Here $\mathbf{r} = r\mathbf{n}$, $\boldsymbol{\varnothing}$ are Pauli matrices, and the profile functions $A$,$B$,$C$,$G$,$H$ can be found numerically by solving the classical equations.

The spherical symmetry of this static solution is preserved under time-independent gauge transformations of the form

$$U(\mathbf{r}) = \exp\Big[iP(r)\,\mathbf{n}\cdot\boldsymbol{\varnothing}\Big] \tag{3.10}$$

with an arbitrary function $P(r)$. One of the five profile functions could be completely eliminated by using this gauge freedom, but since in this case the remaining functions are not necessarily regular at the origin and at infinity, which is required by our numerics, we use all five functions.

It should be mentioned that the expression for the Chern–Simons Number given in eq. (3.3) is not gauge invariant, so it is only well-defined if we require the fields to be continuous at infinity. In this case $N_{\mathrm{CS}}$ is determined up to an integer number which is the winding number of a possible gauge transformation. The final results should be independent of the choice of the gauge. Since we did not exploit the gauge freedom to eliminate one of the five profile functions, we can verify this gauge invariance numerically. This provides a powerful non-trivial check of our performance.

We can rewrite the general Langer–Affleck formula eq. (3.6) in the form

$$\Gamma = \frac{m_W \omega_-}{2\pi}\,\frac{\displaystyle\int \mathcal{D}a\,\mathcal{D}\varphi\,\mathcal{D}\psi^\dagger\mathcal{D}\psi\,\exp\Big(-S[\bar{A}+ga,\bar{\Phi}+g\varphi,\psi^\dagger,\psi]^{\,2^{\mathrm{nd}}}_{\mathrm{order}}\Big)}{\displaystyle\int \mathcal{D}a\,\mathcal{D}\varphi\,\mathcal{D}\psi^\dagger\mathcal{D}\psi\,\exp\Big(-S[\bar{A}^{(0)}+ga,\bar{\Phi}^{(0)}+g\varphi,\psi^\dagger,\psi]^{\,2^{\mathrm{nd}}}_{\mathrm{order}}\Big)}\,. \tag{3.11}$$

Here the Euclidean action

$$\begin{aligned}
S[A,\Phi,\psi^\dagger,\psi] = \frac{1}{g^2}\int_0^{\beta m_W} dt \int d^3\mathbf{r}\Big[&\tfrac{1}{4}(F^a_{\mu\nu})^2 + \tfrac{1}{2}(D_\mu\Phi)^\dagger(D_\mu\Phi) \\
&+ \tfrac{1}{32}\nu_H^2(\Phi^\dagger\Phi-4)^2 + g^2\,(\psi_L^\dagger\ \psi_R^\dagger)\begin{pmatrix} D_0 + i\sigma_i D_i & M \\ M^\dagger & \partial_0 - i\sigma_i\partial_i \end{pmatrix}\binom{\psi_L}{\psi_R}\Big]
\end{aligned} \tag{3.12}$$

is expanded to second order in fluctuations around the sphaleron configuration $\bar{A}, \bar{\Phi}$ in the numerator and around the vacuum configuration $\bar{A}^{(0)}, \bar{\Phi}^{(0)}$ in the denominator. $\beta = 1/T$ is the inverse of the temperature $T$.

In zeroth order (no fluctuations) $S$ reduces to $\beta$ times the classical energy (3.7) of the sphaleron or the vacuum configuration, hence the transition rate $\Gamma$ contains the Boltzmann factor $\exp[-\beta(E_{\rm class} - E^{(0)}_{\rm class})]$ mentioned above, where we have $E^{(0)}_{\rm class} = E_{\rm class}[\bar{A}^{(0)}, \bar{\Phi}^{(0)}] = 0$.

In fact, formula (3.11) should be modified to take into account the gauge fixing, renormalization and special treatment of zero modes. Let us start with the gauge fixing. Following [15] we shall work in the background $R_\xi$ gauge defined by adding the term

$$\tfrac{1}{2}\Big((\bar{D}_\mu a_\mu)^a + \tfrac{i}{4}(\bar{\Phi}^\dagger \tau^a \varphi - \varphi^\dagger \tau^a \bar{\Phi})\Big)^2 \tag{3.13}$$

to the quadratic form for the fluctuations $a$, $\varphi$. $\bar{D}$ is the covariant derivative with the background field $\bar{A}$. In this gauge the Faddeev–Popov determinant is

$$\kappa^2_{\rm FP} = |\det\Big(-\partial_0^2 + \mathcal{K}_{\rm FP}\Big)| \qquad \text{with} \qquad \mathcal{K}_{\rm FP} = -\bar{D}_i^2 + \tfrac{1}{4}\,\bar{\Phi}^\dagger\bar{\Phi}\;. \tag{3.14}$$

The quadratic form of the action expanded about the sphaleron solution in this gauge is

$$\begin{aligned}
\delta^{(2)}S \;=\; & \tfrac{1}{2}\int_0^{\beta m_W} d^4x \,\Big[a^a_\mu\Big(-\partial_0^2 - \bar{D}_i^2 + \tfrac{1}{4}\bar{\Phi}^\dagger\bar{\Phi}\Big)^{ab} a^b_\mu + 2\epsilon^{abc}\bar{F}^c_{ij} a^a_i a^b_j \\
& - i\, a^a_i\Big((\bar{D}_i\bar{\Phi})^\dagger\tau^a\varphi - \varphi^\dagger\tau^a(\bar{D}_i\bar{\Phi})\Big) + \frac{\nu_H^2}{16}(\bar{\Phi}^\dagger\varphi + \varphi^\dagger\bar{\Phi})^2 \\
& - \frac{1}{16}(\bar{\Phi}^\dagger\tau^a\varphi - \varphi^\dagger\tau^a\bar{\Phi})^2 + \varphi^\dagger\Big(-\partial_0^2 - \bar{D}_i^2 + \frac{\nu_H^2}{8}(\bar{\Phi}^\dagger\bar{\Phi} - 4)\Big)\varphi \\
& + 2\,(\psi_L^\dagger\;\psi_R^\dagger)\begin{pmatrix} \partial_0 + i\sigma_i\bar{D}_i & \bar{M} \\ \bar{M}^\dagger & \partial_0 - i\sigma_i\partial_i \end{pmatrix}\begin{pmatrix}\psi_L \\ \psi_R\end{pmatrix}\Big],
\end{aligned} \tag{3.15}$$

where $\bar{M}$ is the mass matrix (2.10) with the background Higgs field $\bar{\Phi}$. The integration over $a_0$ yields the inverse square-root of the Faddeev–Popov determinant, $1/\kappa_{\rm FP}$. The spherical symmetry of the sphaleron solution leads to certain symmetries of the quadratic form of the action. In order to make these symmetries explicit in the Higgs sector, we prefer to work with the complex Higgs doublets in terms of four real components. Any complex doublet $\xi$ can be represented in the form

$$\xi = \begin{pmatrix}\xi_2 + i\xi_1 \\ \xi_4 - i\xi_3\end{pmatrix} = \xi_\mu\tau^+_\mu\begin{pmatrix}0\\1\end{pmatrix} \qquad \text{with} \qquad \tau^\pm_\mu = (\pm i\o, 1) \qquad (\mu = 1,\ldots,4)\;; \tag{3.16}$$

where $\xi_\mu$ is a real four vector. One has

$$\begin{aligned}\xi^\dagger\zeta + \zeta^\dagger\xi &= 2\xi_\mu\zeta_\mu \\ i\,(\xi^\dagger\tau^a\zeta - \zeta^\dagger\tau^a\xi) &= 2\eta^a_{\mu\nu}\xi_\mu\zeta_\nu\end{aligned} \tag{3.17}$$

where $\eta^a_{\mu\nu}$ is the 't Hooft symbol

$$\eta^a_{\mu\nu} = \frac{1}{4i}\,\mathrm{tr}\left[\tau^a(\tau^+_\mu\tau^-_\nu - \tau^+_\nu\tau^-_\mu)\right], \qquad \eta^a_{\mu 4} = -\eta^a_{4\mu} = \delta_{a\mu}\,, \qquad \eta^a_{ij} = \epsilon_{aij}\,. \tag{3.18}$$

In this four component language the covariant derivative $D_\lambda\xi = (D_\lambda\xi)_\mu\tau^+_\mu\binom{0}{1}$ can be written as

$$(D_\lambda\xi)_\mu = (D_\lambda)_{\mu\nu}\xi_\nu \qquad \text{with} \qquad (D_\lambda)_{\mu\nu} = \delta_{\mu\nu}\partial_\lambda - \tfrac{1}{2}\eta^a_{\mu\nu}A^a_\lambda\,. \tag{3.19}$$

Joining the fluctuations of the gauge and Higgs fields into a 13 component vector $(a^a_i\ \varphi_\mu)$ we can rewrite the quadratic form of the action (3.16) in the form

$$\delta^{(2)}S = \int_0^{\beta m_W} d^4x\left[\tfrac{1}{2}(a\ \varphi)(-\partial_0^2 + \mathcal{K}_{\mathrm{bos}})\begin{pmatrix}a\\ \varphi\end{pmatrix} + (\psi^\dagger_L\ \psi^\dagger_R)(\partial_0 + \mathcal{H}_{\mathrm{ferm}})\begin{pmatrix}\psi_L\\ \psi_R\end{pmatrix}\right], \tag{3.20}$$

where

$$\begin{aligned}\mathcal{K}_{\mathrm{bos}} &= \begin{pmatrix}\mathcal{G}^{ab}_{ij} & \mathcal{W}^a_{i\nu}\\ \mathcal{W}^b_{j\mu} & \mathcal{H}_{\mu\nu}\end{pmatrix}, \\ \mathcal{G}^{ab}_{ij} &= \delta_{ij}\Big(-(\bar D^2_k)^{ab} + \tfrac{1}{4}\,\delta^{ab}\bar\Phi_\alpha\bar\Phi_\alpha\Big) + 2\epsilon^{abc}\bar F^c_{ij}\,, \\ \mathcal{H}_{\mu\nu} &= -(\bar D^2_k)_{\mu\nu} - \tfrac{1}{4}(1-\nu_H^2)\bar\Phi_\mu\bar\Phi_\nu + \tfrac{1}{4}\,\delta_{\mu\nu}\Big((1+\tfrac{1}{2}\nu_H^2)\bar\Phi_\alpha\bar\Phi_\alpha - 2\nu_H^2\Big)\,, \\ \mathcal{W}^a_{i\nu} &= \eta^a_{\nu\alpha}(\bar D_i\bar\Phi)_\alpha\,, \\ \mathcal{H}_{\mathrm{ferm}} &= \begin{pmatrix} i\sigma_i\bar D_i & \tfrac{1}{2}\nu_F\bar\Phi_\mu\tau^+_\mu \\ \tfrac{1}{2}\nu_F\bar\Phi_\mu\tau^-_\mu & -i\sigma_i\partial_i\end{pmatrix}.\end{aligned} \tag{3.21}$$

In order to preserve the spherical symmetry of the fermionic Hamiltonian $\mathcal{H}_{\mathrm{ferm}}$ we have taken equal masses for up and down fermions:

$$m_u = m_d\,, \qquad \nu_F = \frac{m_u}{m_W} = \frac{m_d}{m_W}\,. \tag{3.22}$$

The physical significance of this approximation will be discussed later.

Using the quadratic form of the action (3.20) we can perform the functional integral in the Langer–Affleck formula for the transition rate (3.11) and get [5, 8]

$$\Gamma = \frac{m_W\omega_-}{2\pi}\,\frac{8\pi^2V}{(g^2\beta)^3}\,N^3_{\mathrm{tr}}N^3_{\mathrm{rot}}\,\frac{\kappa_{\mathrm{FP}}}{\kappa^{(0)}_{\mathrm{FP}}}\,\frac{\kappa^{(0)}_{\mathrm{bos}}}{\kappa_{\mathrm{bos}}}\,\frac{\kappa_{\mathrm{ferm}}}{\kappa^{(0)}_{\mathrm{ferm}}}\,\exp[-\beta E^{\mathrm{bare}}_{\mathrm{class}}]\,. \tag{3.23}$$

Here $E_{\rm class}^{\rm bare}$ is the classical energy (3.7) of the sphaleron solution with bare (unrenormalized) parameters. The (dimensionful) quantity $V$ is the physical space volume arising from the integration over the three translational zero modes of the sphaleron. Moreover the sphaleron has three rotational zero modes. The effect of all zero modes is taken into account in eq. (3.23) through the factor [13] $\frac{8\pi^2 V}{(g^2\beta)^3}\, N_{\rm tr}^3 N_{\rm rot}^3$ with the Jacobians

$$\begin{aligned} N_{\rm tr} &= \Big[\tfrac{1}{6\pi}\int d^3\mathbf{r}\,\Big((\bar F_{ik}^a)^2 + (\bar D_k\bar\Phi)^\dagger(\bar D_k\bar\Phi)\Big)\Big]^{\frac12} \qquad (3.24)\\ N_{\rm rot} &= \Big[\tfrac{1}{6\pi}\int d^3\mathbf{r}\,\Big((r^2\delta_{jl}-r_jr_l)\Big(\bar F_{ij}^a\bar F_{il}^a + (\bar D_j\bar\Phi)^\dagger(\bar D_l\bar\Phi)\Big) - \epsilon_{kij}\Lambda_k^a\bar F_{ij}^a\Big)\Big]^{\frac12}\,, \end{aligned}$$

where $\Lambda$ is the solution of the equation

$$\Big(-\bar D_l^2 + \tfrac14\bar\Phi^\dagger\bar\Phi\Big)_{ab}\Lambda_k^b = \epsilon_{kij}\bar F_{ij}^a\,. \qquad (3.25)$$

The determinants $\kappa_{\rm FP}$, $\kappa_{\rm bos}$, $\kappa_{\rm ferm}$ in eq. (3.23) arise from the Gaussian integration over fluctuations with periodic time boundary conditions for bosons and antiperiodic boundary conditions for fermions. We can write them in the following form

$$\kappa_{\rm FP} = \Big[\det(-\partial_0^2+\mathcal{K}_{\rm FP})\Big]^{\frac12} = \prod_n\Big(2\sinh(\tfrac{\beta}{2}m_W\omega_n^{\rm FP})\Big) \qquad (3.26)$$

$$\kappa_{\rm bos} = \Big[\det{}'(-\partial_0^2+\mathcal{K}_{\rm bos})\Big]^{\frac12} = \prod_n{}'\Big(2\sinh(\tfrac{\beta}{2}m_W\omega_n)\Big) \qquad (3.27)$$

$$\kappa_{\rm ferm} = \det(\partial_0+\mathcal{H}_{\rm ferm}) = \prod_n\Big(2\cosh(\tfrac{\beta}{2}m_W\varepsilon_n)\Big)\,, \qquad (3.28)$$

where $\omega_n^2, \omega_n^{\rm FP\,2}$, and $\varepsilon_n$ are the eigenvalues of $\mathcal{K}_{\rm bos}, \mathcal{K}_{\rm FP}$, and $\mathcal{H}_{\rm ferm}$, respectively. Our numerics is based on a calculation of the eigenvalues of discretized versions of these operators; details can be found in Appendix A and in [17]. The primed product in eq. (3.27) means that the zero modes are omitted, the negative mode $\omega_-^2$, however, contributes to $\kappa_{\rm bos}$.

# 4 Renormalization

Equation (3.23) for the transition rate contains ultraviolet divergences arising from the infinite products in eqs. (3.26–3.28). These divergences are removed by the renormalization, where it is sufficient to renormalize the theory at zero temperature. Keeping

this in mind we split the right hand side of eq. (3.23) into the temperature dependent finite part and the divergent part corresponding to zero temperature. We write

$$\begin{aligned}\Gamma &= \frac{m_W|\omega_-|}{4\pi\sin(\frac{\beta}{2}m_W|\omega_-|)}\,\frac{8\pi^2V}{g^6\beta^3}\,(N_{\rm tr}N_{\rm rot})^3\,\exp\Big[-\beta\Big(E^{\rm bare}_{\rm class} \\ &\quad + E^{T=0}_{\rm FP} + E^{\rm temp}_{\rm FP}(T) + E^{T=0}_{\rm bos} + E^{\rm temp}_{\rm bos}(T) + E^{T=0}_{\rm ferm} + E^{\rm temp}_{\rm ferm}(T)\Big)\Big]\,,\end{aligned} \tag{4.1}$$

where the ultraviolet divergent $T=0$ terms are

$$\begin{aligned}E^{T=0}_{\rm FP} &= -\tfrac{1}{2}m_W\Big(\sum_n \omega_n^{\rm FP} - \sum_n \omega_n^{{\rm FP}\,0}\Big)\,, \\ E^{T=0}_{\rm bos} &= +\tfrac{1}{2}m_W\Big(\sum_n{}'' \omega_n - \sum_n \omega_n^{0}\Big)\,, \\ E^{T=0}_{\rm ferm} &= -\tfrac{1}{2}m_W\Big(\sum_n |\varepsilon_n| - \sum_n |\varepsilon_n^0|\Big)\,.\end{aligned} \tag{4.2}$$

The temperature dependent terms

$$\begin{aligned}E^{\rm temp}_{\rm FP}(T) &= -\tfrac{1}{\beta}\Big(\sum_n \ln(1-e^{-\beta m_W\omega_n^{\rm FP}}) - \sum_n \ln(1-e^{-\beta m_W\omega_n^{{\rm FP}\,0}})\Big)\,, \\ E^{\rm temp}_{\rm bos}(T) &= +\tfrac{1}{\beta}\Big(\sum_n{}'' \ln(1-e^{-\beta m_W\omega_n}) - \sum_n \ln(1-e^{-\beta m_W\omega_n^{0}})\Big)\,, \\ E^{\rm temp}_{\rm ferm}(T) &= -\tfrac{1}{\beta}\Big(\sum_n \ln(1+e^{-\beta m_W|\varepsilon_n|}) - \sum_n \ln(1+e^{-\beta m_W|\varepsilon_n^0|})\Big)\end{aligned} \tag{4.3}$$

are finite and vanish at zero temperature. Here $\sum''$ stands for the sum over all non-zero, non-negative modes.

We shall perform the renormalization of the zero-temperature contribution using the proper-time representation for the quantities (4.2) with the cutoff parameter $\Lambda$:

$$E^{T=0}_{\rm FP}(\Lambda) = \frac{m_W}{4\sqrt{\pi}}\int_{\Lambda^{-2}}^\infty \frac{dt}{t^{3/2}}\,{\rm Tr}\,\Big(\exp[-t\mathcal{K}_{\rm FP}] - \exp[-t\mathcal{K}^{(0)}_{\rm FP}]\Big)\,, \tag{4.4}$$

$$E^{T=0}_{\rm ferm}(\Lambda) = \frac{m_W}{4\sqrt{\pi}}\int_{\Lambda^{-2}}^\infty \frac{dt}{t^{3/2}}\,{\rm Tr}\,\Big(\exp[-t\mathcal{H}^2_{\rm ferm}] - \exp[-t(\mathcal{H}^{(0)}_{\rm ferm})^2]\Big)\,. \tag{4.5}$$

In the case of $E^{T=0}_{\rm bos}$ the proper time representation is modified to suppress the negative mode contribution:

$$E^{T=0}_{\rm bos}(\Lambda) = -\frac{m_W}{4\sqrt{\pi}}\int_{\Lambda^{-2}}^\infty \frac{dt}{t^{3/2}}\,\Big\{\,{\rm Tr}\,\Big(\exp[-t\mathcal{K}_{\rm bos}] - \exp[-t\mathcal{K}^{(0)}_{\rm bos}]\Big) + (1-e^{-t\omega_-^2})\Big\} \tag{4.6}$$

In the limit $\Lambda\to\infty$ these integrals diverge since for $t\to 0$

$${\rm Tr}\,\Big(\exp[-t\mathcal{K}] - \exp[-t\mathcal{K}^{(0)}]\Big) = at^{-1/2} + bt^{1/2} + \cdots\,, \tag{4.7}$$

where $\mathcal{K}$ can stand for $\mathcal{K}_{\rm bos}, \mathcal{K}_{\rm FP}, \mathcal{K}_{\rm ferm} = \mathcal{H}^2_{\rm ferm}$. We write the divergent pieces of the r.h.s. of eqs. (4.4–4.6) as

$$
\begin{aligned}
E^{\rm div}_{\rm FP} &= \frac{m_W}{4\sqrt{\pi}} \int_{\Lambda^{-2}}^{\nu_{\rm ren}^{-2}} \frac{dt}{t^{3/2}} \left[ \,{\rm Tr}\, \exp(-t\mathcal{K}_{\rm FP}) \right]_{\rm div} , \\
E^{\rm div}_{\rm bos} &= -\frac{m_W}{4\sqrt{\pi}} \int_{\Lambda^{-2}}^{\nu_{\rm ren}^{-2}} \frac{dt}{t^{3/2}} \left[ \,{\rm Tr}\, \exp(-t\mathcal{K}_{\rm bos}) \right]_{\rm div} , \\
E^{\rm div}_{\rm ferm} &= \frac{m_W}{4\sqrt{\pi}} \int_{\Lambda^{-2}}^{\nu_{\rm ren}^{-2}} \frac{dt}{t^{3/2}} \left[ \,{\rm Tr}\, \exp(-t\mathcal{K}_{\rm ferm}) \right]_{\rm div} ,
\end{aligned}
\tag{4.8}
$$

where we define

$$
\left[ \,{\rm Tr}\, \exp(-t\mathcal{K}) \right]_{\rm div} = a t^{-1/2} + b t^{1/2} , \tag{4.9}
$$

and $\nu_{\rm ren} m_W$ is the renormalization scale which is determined below from the value of the Higgs pole mass. Performing the small $t$ expansion (4.7) and integrating over $t$ in (4.8) we find

$$
\begin{aligned}
E^{\rm div}_{\rm FP}(\Lambda) &= \frac{m_W}{64\pi^2} \int d^3\mathbf{r} \left[ \tfrac{3}{2}(\nu^2_{\rm ren} - \Lambda^2)(\bar\Phi^\dagger\bar\Phi - 4) \right. \\
&\qquad \left. + \ln\left(\tfrac{\Lambda^2}{\nu^2_{\rm ren}}\right) \left( -\tfrac{1}{3}(\bar F^a_{ij})^2 + \tfrac{3}{16}(\bar\Phi^\dagger\bar\Phi - 4)^2 + \tfrac{3}{2}(\bar\Phi^\dagger\bar\Phi - 4) \right) \right] , \\
E^{\rm div}_{\rm bos}(\Lambda) &= -\frac{m_W}{64\pi^2} \int d^3\mathbf{r} \left[ \tfrac{3}{2}(\nu^2_{\rm ren} - \Lambda^2)(4 + \nu_H^2)(\bar\Phi^\dagger\bar\Phi - 4) + \ln\left(\tfrac{\Lambda^2}{\nu^2_{\rm ren}}\right) \left( \tfrac{41}{6}(\bar F^a_{ij})^2 \right. \right. \\
&\qquad \left. \left. + 6(\bar D_i\bar\Phi)^\dagger(\bar D_i\bar\Phi) + \tfrac{3}{16}(4 + \nu_H^2 + \nu_H^4)(\bar\Phi^\dagger\bar\Phi - 4)^2 + \tfrac{3}{4}(8 + \nu_H^2 + \nu_H^4)(\bar\Phi^\dagger\bar\Phi - 4) \right) \right] , \\
E^{\rm div}_{\rm ferm}(\Lambda) &= \frac{m_W}{64\pi^2} \sum_F \int d^3\mathbf{r} \left[ 4\nu_F^2(\nu^2_{\rm ren} - \Lambda^2)(\bar\Phi^\dagger\bar\Phi - 4) + \ln\left(\tfrac{\Lambda^2}{\nu^2_{\rm ren}}\right) \left( \tfrac{1}{3}(\bar F^a_{ij})^2 \right. \right. \\
&\qquad \left. \left. + 2\nu_F^2(\bar D_i\bar\Phi)^\dagger(\bar D_i\bar\Phi) + \tfrac{1}{2}\nu_F^4(\bar\Phi^\dagger\bar\Phi - 4)^2 + 4\nu_F^4(\bar\Phi^\dagger\bar\Phi - 4) \right) \right] .
\end{aligned}
\tag{4.10}
$$

The fermionic part in the above formulas is written for one fermion doublet. As it was mentioned above, to preserve the spherical symmetry of the Dirac equation one has to consider the case of equal masses for up and down fermions. This approximation is justified for doublets where both fermions are light. However, in the case of the $(t, b)$ doublet the approximation $m_b \ll m_W \ll m_t$ is more reasonable. In this limit the correction from the top quark is *half* that of the doublet with both masses equal to $m_t$ [17]. Therefore, in our numerical estimates we take $9 + \frac{3}{2}$ massless fermion doublets and $\frac{3}{2}$ massive doublets with mass $m_t$, taking into account that the quark contribution is enhanced by three colours.

We see that the quadratically ($\Lambda^2$) and logarithmically ($\ln\Lambda^2$) divergent terms are exactly those entering the classical energy functional $E^{\rm bare}_{\rm class}$ (3.7). Therefore, they

can be combined with the bare constants of the correspondent terms in the classical energy — to produce the renormalized constants at the scale of $\nu_{\rm ren} m_W$. We call the classical energy with renormalized constants $E_{\rm class}$.

What is left after the renomalization is ultraviolet finite, and one can safely put the ultraviolet cutoff $\Lambda$ to infinity. We call these pieces renormalized energies,

$$E^{\rm ren}_{\rm FP} = \lim_{\Lambda\to\infty} E^{\rm conv}_{\rm FP}(\Lambda)\,, \tag{4.11}$$

with

$$\begin{aligned} E^{\rm conv}_{\rm FP}(\Lambda) &= \frac{m_W}{4\sqrt{\pi}}\Bigg[\int_{\Lambda^{-2}}^{\infty}\frac{dt}{t^{3/2}}\,{\rm Tr}\left(\exp[-t\mathcal{K}_{\rm FP}]-\exp[-t\mathcal{K}^{(0)}_{\rm FP}]\right) \\ &\qquad -\int_{\Lambda^{-2}}^{\nu_{\rm ren}^{-2}}\frac{dt}{t^{3/2}}\,[\,{\rm Tr}\,\exp(-t\mathcal{K}_{\rm FP})]_{\rm div}\Bigg]\,, \end{aligned} \tag{4.12}$$

and similarly for $E^{\rm ren}_{\rm ferm}$ and $E^{\rm ren}_{\rm bos}$. In the case of $E^{\rm ren}_{\rm bos}$ one should take into account the subtraction of the negative mode contribution in (4.6) so that

$$\begin{aligned} E^{\rm conv}_{\rm bos}(\Lambda) &= -\frac{m_W}{4\sqrt{\pi}}\Bigg[\int_{\Lambda^{-2}}^{\infty}\frac{dt}{t^{3/2}}\left[\,{\rm Tr}\left(\exp[-t\mathcal{K}_{\rm bos}]-\exp[-t\mathcal{K}^{(0)}_{\rm bos}]\right)+(1-e^{-t\omega_-^2})\right] \\ &\qquad -\int_{\Lambda^{-2}}^{\nu_{\rm ren}^{-2}}\frac{dt}{t^{3/2}}\,[\,{\rm Tr}\,\exp(-t\mathcal{K}_{\rm bos})]_{\rm div}\Bigg]\,. \end{aligned} \tag{4.13}$$

Performing the described renormalization procedure we arrive at the following expression for the transition rate (4.1)

$$\begin{aligned} \gamma &= \frac{\Gamma}{V} = \frac{2\pi m_W|\omega_-|(N_{\rm tr}N_{\rm rot})^3}{g^6\beta^3\sin(\frac{\beta}{2}m_W|\omega_-|)}\,\exp\Big[-\beta\Big(E_{\rm class}+E^{\rm ren}_{\rm FP}+E^{\rm temp}_{\rm FP}(T) \\ &\qquad +E^{\rm ren}_{\rm bos}+E^{\rm temp}_{\rm bos}(T)+E^{\rm ren}_{\rm ferm}+E^{\rm temp}_{\rm ferm}(T)\Big)\Big]\,. \end{aligned} \tag{4.14}$$

Finally we fix the renormalization point $\nu_{\rm ren}$ in eqs. (4.8, 4.12, 4.13) so that the renormalized parameter $\nu_H$ coincides with the physical pole mass. In order to obtain the pole mass we have to evaluate the propagator of the Higgs particle in one-loop order. Its classical part (in Euclidean space) is given by $G^{-1}(p^2) = p^2 + \nu_H^2$ (in units of $m_W^2$), the fermionic and bosonic one-loop corrections can be written as $\alpha\, N_c\, \nu_t^4\, F_{\rm ferm}(\frac{\nu^2_{\rm ren}}{\nu_t^2},\, \frac{p^2}{\nu_t^2})$ and $\alpha\, \nu^2_{\rm ren}\, F_{\rm bos}(\nu^2_{\rm ren},\, p^2,\, \nu_H^2)$ with some functions $F_{\rm ferm}$ and $F_{\rm bos}$ which are finite in the limit of infinite $\nu_t$ and $\nu_{\rm ren}$, respectively.

In most parts of our numerical computation we work with a top quark mass substantially larger than $m_H$. From the classical part of $G^{-1}(p^2)$ we know that $p^2$ is

of the order of $-\nu_H^2$, while we find (see below) $\nu_{\rm ren}^2 \sim \nu_t^2$. Therefore, the dominating parts of the one loop contribution are terms of the order $\alpha\, N_c \nu_t^4$ and $\alpha\, N_c \nu_t^2$ stemming from the fermionic correction, so for $m_t$ significantly larger than $m_H$ it is a good approximation to drop the bosonic contribution completely (its leading term is only of the order $\alpha\, \nu_{\rm ren}^2 \sim \alpha\, \nu_t^2$) and to expand $F_{\rm ferm}$ in $p^2/\nu_t^2$ up to the order $\mathcal{O}(p^2/\nu_t^2)$. Within this approximation we can also neglect corrections to the pole mass of the W-boson. Exceptions from this procedure will be treated below.

In order to get the Higgs propagator we put the gauge field to zero and obtain the relevant (four-dimensional) action:

$$S = S_0 + S_{\rm loop}\,, \tag{4.15}$$

with

$$\begin{aligned} S_0 &= \frac{1}{g^2}\int d^4x \left[\tfrac{1}{2}(\partial_\mu\Phi)^\dagger(\partial_\mu\Phi) + \tfrac{\nu_H^2}{32}(\Phi^\dagger\Phi)^2 - \tfrac{\nu_H^2}{4}\Phi^\dagger\Phi\right], \qquad (4.16)\\ S_{\rm loop} &= -\frac{1}{2}\,{\rm Tr}\,\log D^\dagger D + S_{\rm counter} = \frac{1}{2}\int_{\Lambda^{-2}}^{\infty}\frac{dt}{t}\;{\rm Tr}\;e^{-tD^\dagger D} - \frac{1}{4\sqrt{\pi}}\int_{\Lambda^{-2}}^{\nu_{\rm ren}^{-2}}\frac{dt}{t}\left(\frac{a}{t}+b\right), \end{aligned}$$

where we used

$$D^\dagger D = -\partial^2 + i\Big[(i\gamma_0\partial_0 + \gamma_i\partial_i)(M\tfrac{1+\gamma_5}{2} + M^\dagger\tfrac{1-\gamma_5}{2})\Big] + M^\dagger M\,, \tag{4.17}$$

and the counterterms

$$a = -\frac{N_c\,\nu_t^2}{8\pi^{3/2}}\int d^4x\,\Phi^\dagger\Phi\,, \qquad b = \frac{N_c}{64\pi^{3/2}}\int d^4x\left(\nu_t^4(\Phi^\dagger\Phi)^2 + 4\nu_t^2(\partial_\mu\Phi)^\dagger(\partial_\mu\Phi)\right). \tag{4.18}$$

The vacuum expectation value of the Higgs field in one-loop order is obtained by setting $\Phi^\dagger\Phi = v^2 = {\rm const}$ in the action (4.15) and minimizing it with respect to $v$. The result up to order $g^2$ is

$$v^2 = v_0^2 + \frac{g^2\,N_c}{2\pi^2\nu_H^2}\left(\nu_t^2\nu_{\rm ren}^2 - \nu_t^4(1 - C - \ln\tfrac{\nu_t^2}{\nu_{\rm ren}^2})\right), \tag{4.19}$$

where $v_0^2 = 4$ is the vev. on the classical level and $C \approx 0.577$ the Euler constant. Choosing the unitary gauge, we can substitute

$$\Phi = \begin{pmatrix} 0 \\ v + g\eta \end{pmatrix}. \tag{4.20}$$

The propagator is then given by

$$\frac{\delta^2 S}{\delta\eta(x_1)\,\delta\eta(x_2)}\Big|_{\eta=0} = \int \frac{d^4p}{(2\pi)^4}\, e^{ip(x_2-x_1)}\, G^{-1}(p^2)\,, \tag{4.21}$$

and we obtain up to order $g^2$

$$G^{-1}(p^2) = p^2 + \nu_H^2 + \frac{g^2\, N_c\, \nu_t^4}{8\pi^2}\left[\tfrac{\nu_{\rm ren}^2}{\nu_t^2} - 1 - \tfrac{1}{4}\,\tfrac{p^2}{\nu_t^2}(C + \ln\tfrac{\nu_t^2}{\nu_{\rm ren}^2}) - (2 + \tfrac{1}{2}\,\tfrac{p^2}{\nu_t^2}) f(-\tfrac{p^2}{\nu_t^2})\right] \tag{4.22}$$

with the function

$$f(x) \equiv \tfrac{1}{2}\int_0^1 d\beta\, \ln|1-\beta(1-\beta)x| = -1 + {\rm Re}\left(\sqrt{\frac{x-4}{x}}\,{\rm artanh}\,\sqrt{\frac{x}{x-4}}\right)\,. \tag{4.23}$$

As mentioned before, we expand the propagator up to terms of $\mathcal{O}(p^2/\nu_t^2)$. We obtain

$$G^{-1}(p^2) = p^2 + \nu_H^2 + \frac{g^2\, N_c\, \nu_t^4}{8\pi^2}\left[\tfrac{\nu_{\rm ren}^2}{\nu_t^2} - 1 - \tfrac{1}{4}\,\tfrac{p^2}{\nu_t^2}\big(\tfrac{2}{3} + C + \ln\tfrac{\nu_t^2}{\nu_{\rm ren}^2}\big)\right]. \tag{4.24}$$

Our aim is to fix $\nu_{\rm ren}$ such that the pole mass $\nu_p$, defined by $G^{-1}(p^2 = -\nu_p^2) = 0$, coincides with $\nu_H$. Hence we have to solve the equation

$$\nu_{\rm ren}^2 = \nu_t^2 - \frac{\nu_H^2}{4}\big(\frac{2}{3} + C + \ln\frac{\nu_t^2}{\nu_{\rm ren}^2}\big) \tag{4.25}$$

which determines the renormalization constant $\nu_{\rm ren}$ for given values of $\nu_t$ and $\nu_H$, $\nu_t \gtrsim \nu_H$. As anticipated, we find $\nu_{\rm ren}^2 \sim \nu_t^2$.

Analogous equations follow from the full (non-expanded) propagator (4.22) and from the propagator which includes both fermionic and bosonic fluctuations. We have checked that for $\nu_t \gtrsim \nu_H$ the results for $\nu_{\rm ren}$ obtained with those equations are very close to the solutions of eq. (4.25), so that in this case the restriction to the dominating parts up to $\mathcal{O}(\alpha\, N_c \nu_t^2)$ is a very good approximation, and for our choice of $\nu_{\rm ren}$ the renormalized parameter $\nu_H$ corresponds to the Higgs pole mass very accurately.

The situation is slightly worse for the case of very large $\nu_H$ (e.g. $m_H = 350$ GeV). Here no solution of eq. (4.25) can be found, so we choose $\nu_{\rm ren}$ such that the difference $|\nu_p - \nu_H|$ takes its minimum. The deviation, however, is found to be below 10%. Moreover, we consider such high Higgs masses only for comparison to our main results, so that this problem is actually irrelevant.

# 5 Thermal renormalization and spectral densities

We next consider the temperature dependent terms in the exponent of (4.1) given by (4.3). In order to compute these quantities we introduce spectral densities $\varrho^{\cdots}(E)$ for the continuous parts of the spectra of the operators $\mathcal{K}_{\cdots}$, such that for any function $f(x)$ that vanishes fast enough for $x \to \infty$ we have

$$\mathrm{Tr}\left(f(\mathcal{K}) - f(\mathcal{K}^{(0)})\right) = \sum_{\substack{\text{dicrete}\\ \text{levels}}} f(\omega^2) + \int_0^\infty dE\ \varrho(E) f(E^2)\ . \tag{5.1}$$

$\mathcal{K}_{\mathrm{bos}}$ has $n_D^{\mathrm{bos}} = 7$ discrete levels (six zero-modes and one negative mode), $\mathcal{K}_{\mathrm{ferm}}$ has $n_D^{\mathrm{ferm}} = 1$ discrete zero mode [17], $\mathcal{K}_{\mathrm{FP}}$ has $n_D^{\mathrm{FP}} = 0$ discrete modes, which by definition are not included in the spectral densities $\varrho^{\cdots}$.

We rewrite eq. (4.3) with the help of the spectral densities:

$$\begin{aligned} E^{\mathrm{temp}}_{\mathrm{bos,FP}}(T) &= \pm\tfrac{1}{\beta}\int_0^\infty dE\ \varrho^{\mathrm{bos,FP}}(E)\ \ln(1 - e^{-\beta m_W E})\ , \\ E^{\mathrm{temp}}_{\mathrm{ferm}}(T) &= -\tfrac{1}{\beta}\int_0^\infty dE\ \varrho^{\mathrm{ferm}}(E)\ \ln(1 + e^{-\beta m_W E}) - \tfrac{1}{\beta}\, n_D^{\mathrm{ferm}} \ln 2\ , \end{aligned} \tag{5.2}$$

where the signs are chosen according to those of $E^{\mathrm{temp}}_{\cdots}(T)$ given in eq. (4.3).

At high temperatures eq. (5.2) is dominated by spectral densities at large energies. It is shown in Appendix B that asymptotically all three spectral densities $\varrho^{\mathrm{FP}}$, $\varrho^{\mathrm{bos}}$ and $\varrho^{\mathrm{ferm}}$ approach constant values (after subtraction of the spectral densities of free operators, which is implied in the definition (5.1)),

$$\lim_{E\to\infty} \varrho(E) = \varrho_\infty\ .$$

Therefore, at high $T$ the quantities $E^{\mathrm{temp}}_{\cdots}(T)$ have a $T^2$ behaviour:

$$E^{\mathrm{large}}_{\cdots}(T) = \pm\tfrac{1}{\beta}\int_0^\infty dE\ \varrho^{\cdots}_\infty \ln(1 \pm e^{-\beta m_W E}) = \pm\frac{\pi^2 \varrho^{\cdots}_\infty T^2}{24 m_W}\,(-1 \pm 3)\ , \tag{5.3}$$

whereas the remaining part of $E^{\mathrm{temp}}_{\cdots}(T)$ can be written as (see eq. (B.13))

$$\begin{aligned} &\pm\tfrac{1}{\beta}\int_0^\infty dE\left(\varrho^{\mathrm{bos,FP}}(E) - \varrho^{\mathrm{bos,FP}}_\infty\right)\ln(1 - e^{-\beta m_W E}) \\ &\quad= \pm\tfrac{1}{\beta}\int_0^\infty dE\left(\varrho^{\mathrm{bos,FP}}(E) - \varrho^{\mathrm{bos,FP}}_\infty\right)\ln\frac{1 - e^{-\beta m_W E}}{\beta m_W} \mp \tfrac{1}{\beta} n_D^{\mathrm{bos,FP}} \ln(\beta m_W) \\ &\quad\equiv E^{\mathrm{small}}_{\mathrm{bos,FP}} \mp \tfrac{1}{\beta} n_D^{\mathrm{bos,FP}} \ln(\beta m_W) \end{aligned} \tag{5.4}$$

$$E^{\mathrm{small}}_{\mathrm{ferm}} = -\tfrac{1}{\beta}\int_0^\infty dE\left(\varrho^{\mathrm{ferm}}(E) - \varrho^{\mathrm{ferm}}_\infty\right)\ln(1 + e^{-\beta m_W E}) - \tfrac{1}{\beta} n_D^{\mathrm{ferm}} \ln 2\ . \tag{5.5}$$

With these definitions the $E^{\rm small}_{...}$ are finite in the high temperature limit (see App. B).

We notice that at $T = \mathcal{O}(m_W/g)$ the local functionals $E^{\rm large}_{...}(T)$ can be of the same order as the (renormalized) classical zero-temperature energy of the sphaleron, therefore in that range of temperature one has to find a new sphaleron solution which is a saddle point of the temperature dependent functional

$$E^{\rm ren}_{\rm class}(T) = E_{\rm class} + E^{\rm large}_{\rm FP}(T) + E^{\rm large}_{\rm bos}(T) + E^{\rm large}_{\rm ferm}(T) \; . \tag{5.6}$$

Fortunately this functional has the same form as the original $E_{\rm class}$, but with temperature dependent parameters. Therefore its saddle point will be just a rescaled version of the original sphaleron configuration.

Using the expressions for $\varrho_\infty$ computed in appendix B eqs. (B.8, B.4) we arrive at

$$\begin{aligned} E^{\rm ren}_{\rm class}[A,\Phi;T] &= \frac{m_W}{g^2}\int d^3\mathbf{r}\left[\tfrac{1}{4}(F^a_{ij})^2 + \tfrac{1}{2}(D_i\Phi)^\dagger(D_i\Phi) + \tfrac{1}{32}\nu_H^2(\Phi^\dagger\Phi-4)^2 \right. \\ &\qquad \left. + \frac{g^2T^2}{32m_W^2}(\tfrac{2}{3}N_c\nu_t^2 + \nu_H^2 + 3)(\Phi^\dagger\Phi - 4)\right] \\ &= \frac{m_W}{g^2}\int d^3\mathbf{r}\left[\tfrac{1}{4}(F^a_{ij})^2 + \tfrac{1}{2}(D_i\Phi)^\dagger(D_i\Phi) + \tfrac{1}{32}\nu_H^2(\Phi^\dagger\Phi-4q^2)^2 \right. \\ &\qquad \left. - \tfrac{1}{32}\nu_H^2(4-4q^2)^2\right] \\ &= \frac{m_W q}{g^2}\int d^3\mathbf{r}\left[\tfrac{1}{4}(\tilde F^a_{ij})^2 + \tfrac{1}{2}(\tilde D_i\tilde\Phi)^\dagger(\tilde D_i\tilde\Phi) + \tfrac{1}{32}\nu_H^2(\tilde\Phi^\dagger\tilde\Phi-4)^2 \right. \\ &\qquad \left. - \tfrac{1}{32}\nu_H^2(4q^{-2}-4)^2\right] \end{aligned} \tag{5.7}$$

where in the last expression we change the integration variable, $\mathbf{r} \to q^{-1}\mathbf{r}$, and use the notations

$$\tilde A(\mathbf{r}) = q^{-1}A(q^{-1}\mathbf{r}) \; , \qquad\qquad \tilde\Phi(\mathbf{r}) = q^{-1}\Phi(q^{-1}\mathbf{r}) \tag{5.8}$$

with (compare e.g. [23])

$$\begin{aligned} q = q(T) &= \sqrt{1-\left(\frac{T}{T_c}\right)^2} \; , \\ T_c &= \frac{2\sqrt{2}\,\nu_H m_W}{g}\left(\tfrac{2}{3}N_c\nu_t^2 + \nu_H^2 + 3\right)^{-\frac{1}{2}} \; . \end{aligned} \tag{5.9}$$

The new temperature dependent sphaleron configuration $\bar A^q, \bar\Phi^q$ which is the saddle point of $E^{\rm ren}_{\rm class}(T)$ can be expressed in terms of the old zero temperature solution $\bar A, \bar\Phi$:

$$\bar A^q(\mathbf{r}) = q\bar A(q\mathbf{r}) \; , \qquad\qquad \bar\Phi^q(\mathbf{r}) = q\bar\Phi(q\mathbf{r}) \; . \tag{5.10}$$

Subtracting the vacuum contribution we find

$$E^{\rm ren}_{\rm class}[\bar{A}^q,\bar{\Phi}^q;T] - E^{\rm ren}_{\rm class}[\bar{A}^{q\,(0)},\bar{\Phi}^{q\,(0)};T] = qE_{\rm class}[\bar{A},\bar{\Phi}]\;. \tag{5.11}$$

If we now replace $\bar{A},\bar{\Phi}$ by $\bar{A}^q,\bar{\Phi}^q$ in all parts of our expression for $\gamma$, we find that we get the old results again but with $m_W$ replaced by $qm_W$ wherever it appears (except in the definition (5.9) of $T_c$). The vacuum expectation value of the Higgs field becomes temperature dependent; it is given by $\Phi^{q\,(0)} = 2q\binom{0}{1}$ and vanishes for $T \to T_c$.

Thus the final result for the transition rate per volume is

$$\begin{aligned}\gamma &= \frac{2\pi q m_W|\omega_-|(N_{\rm tr}N_{\rm rot})^3}{g^6\beta^3\sin(\frac{\beta}{2}qm_W|\omega_-|)}\,(qm_W\beta)^{n_D^{\rm bos}}\,\exp\Big[-\beta q\Big(E_{\rm class}+E^{\rm ren}_{\rm FP}+E^{\rm ren}_{\rm bos}+E^{\rm ren}_{\rm ferm}\Big)\\ &\qquad -\beta\Big(E^{\rm small}_{\rm FP}(T)+E^{\rm small}_{\rm bos}(T)+E^{\rm small}_{\rm ferm}(T)\Big)_{\,m_W\to qm_W}\Big]\\ &= \mathcal{F}\exp\Big[-\beta\Big(qE_{\rm class}+E_{\rm FERM}+E_{\rm BOS}\Big)\Big]\end{aligned} \tag{5.12}$$

with the prefactor

$$\mathcal{F} = \frac{2\pi(qm_W)^8\beta^4|\omega_-|(N_{\rm tr}N_{\rm rot})^3}{g^6\sin(\frac{\beta}{2}qm_W|\omega_-|)}\,, \tag{5.13}$$

and the total fermionic and bosonic one-loop contributions are

$$\begin{aligned}E_{\rm FERM} &= qE^{\rm ren}_{\rm ferm}+E^{\rm small}_{\rm ferm}(T)\Big|_{qm_W}\\ E_{\rm BOS} &= qE^{\rm ren}_{\rm bos}+E^{\rm small}_{\rm bos}(T)\Big|_{qm_W}+qE^{\rm ren}_{\rm FP}+E^{\rm small}_{\rm FP}(T)\Big|_{qm_W}\;.\end{aligned} \tag{5.14}$$

# 6 Dissipation of the baryon asymmetry

In this section we express the erasure of the BAU after the electroweak phase transition through the transition rate $\gamma(T)$ following the considerations of [8] (see also [5]).

Transitions over the sphaleron barrier change the baryon and lepton number by $\Delta B = \Delta L = N_g\,\Delta N_{\rm CS}$, where $N_g = 3$ is the number of generations.

If there were neither baryons nor leptons initially, the transitions increasing $N_{\rm CS}$ would be compensated by processes decreasing $N_{\rm CS}$ so that creation and annihilation of baryons would cancel each other. The situation becomes different, however, if we assume the initial existence of baryons and leptons. These particles could have been created long time before the electroweak phase transtion in the age of GUT or maybe

during the phase transition. In this case the chemical potentials $\mu$ of the baryons and leptons are non-zero which leads to an additional term $\mu N_{\rm CS}$ in the classical energy functional. In accordance with the Le Châtelier principle the transitions will favor the wash-out of any particle or antiparticle excess.

Our analysis will be restricted to the usual electroweak theory where $B-L$ is conserved. Therefore, the study of the erasure of the BAU in the context of sphaleron transitions makes sense only under the assumption of the initial condition $B=L$.

A sphaleron transition with $\Delta N_{\rm CS}=1$ creates one particle per fermion doublet. We introduce chemical potentials $\mu_i^Q$ $(i=1,\ldots,9)$ for the quark doublets and $\mu_i^L$ $(i=1,\ldots,3)$ for the lepton doublets. Then each transition increases the energy by $\Delta N_{\rm CS}\left(\sum_{i=1}^9 \mu_i^Q + \sum_{i=1}^3 \mu_i^L\right)$, i.e. the classical energy functional (3.7) has to be replaced by [24, 25]

$$E_{\rm class} \to E_{\rm class} + N_{\rm CS}\left(\sum_{i=1}^9 \mu_i^Q + \sum_{i=1}^3 \mu_i^L\right) . \tag{6.1}$$

This $\mu$ contribution leads to the asymmetry in the Langer–Affleck formula (5.12) with respect to transitions increasing and decreasing $N_{\rm CS}$. We have to set $N_{\rm CS}=+\frac{1}{2}$ for transitions which increase the fermion number and $N_{\rm CS}=-\frac{1}{2}$ for transitions which decrease it. Since the baryon and lepton densities considered are very small we can restrict the transition rate to terms linear in $\mu$

$$\begin{aligned}
\gamma_+ &= \gamma\left[1-\frac{\beta}{2}\left(\sum_{i=1}^9 \mu_i^Q + \sum_{i=1}^3 \mu_i^L\right)\right] , \\
\gamma_- &= \gamma\left[1+\frac{\beta}{2}\left(\sum_{i=1}^9 \mu_i^Q + \sum_{i=1}^3 \mu_i^L\right)\right] ,
\end{aligned} \tag{6.2}$$

so that the baryon and lepton number dissipation, given by the difference of these rates, reads:

$$\frac{dB}{dt} = \frac{dL}{dt} = -\gamma(T)\, V N_g\, \beta\left(\sum_{i=1}^9 \mu_i^Q + \sum_{i=1}^3 \mu_i^L\right) . \tag{6.3}$$

Now we have to express the chemical potentials through the particle numbers in order to get a differential equation for the baryon number decrease. For small $\mu$ standard Fermi–Dirac statistics yields the relation

$$N(\mu) = \frac{fV}{6\beta^2}\, I(\beta m)\, \mu\,, \tag{6.4}$$

where $N$ is the number of fermions, $f$ the number of degrees of freedom, $m$ the mass of the fermions and $I(a)$ is given by

$$I(a) = \frac{12}{\pi^2} \int_a^\infty \frac{dx}{1+e^x} \frac{x^2 - \frac{1}{2}a^2}{\sqrt{x^2 - a^2}}, \tag{6.5}$$

with the properties $I(0) = 1$, $I(\infty) = 0$. A lepton doublet has three degrees of freedom (two for the lepton and one for the neutrino) while there are four for a quark doublet. The masses of the leptons and the light quarks are much smaller than the critical temperature $T_c = 1/\beta_c$, i.e. $\beta_c m \ll 1$ so that $I(\beta_c m) \approx 1$. We apply this approximation also in the case of the top quark since it has almost no influence on the result for the baryon number wash-out. Hence we obtain for the lepton and the light quark doublets:

$$\mu_i^L = \frac{2\beta^2}{V} L_i, \qquad \mu_i^Q = \frac{3\beta^2}{2V} Q_i, \tag{6.6}$$

where $L_i$, $Q_i$ are the numbers of leptons and quarks of a fixed doublet $i$. Substituting eq. (6.6) into eq. (6.3) and using $L = B = Q/3$ we obtain:

$$\frac{dB}{dt} = -\gamma(T)\, V N_g\, \beta \left\{ \frac{3\beta^2}{2V} Q + \frac{2\beta^2}{V} L \right\} = -\tfrac{13}{2}\, \gamma(T)\, N_g\, \beta^3 B\,. \tag{6.7}$$

Standard cosmology gives a relation between time and temperature [26, 27]:

$$t = \sqrt{\frac{45}{16\pi^3 N(T)}}\, m_P T^{-2} = C\, T^{-2}, \tag{6.8}$$

where $N(T)$ is some number related to the number of degrees of freedom of the thermalized particles at the temperature $T$ (for our range of temperature it is usually $\frac{381}{4}$), $m_P = 1.5 \cdot 10^{17}\, m_W$ is the Planck mass and hence the constant $C$ is given by $C \approx 5 \cdot 10^{15}\, m_W$. Substitution yields

$$\frac{1}{B}\frac{dB}{dT} = 13 N_g\, C\, \frac{\gamma(T)}{T^6}, \tag{6.9}$$

which can be integrated to

$$\begin{aligned} B(T) &= B(T_c)\, \exp\left\{ -13 N_g\, C \int_T^{T_c} \frac{\gamma(T)}{T^6}\, dT \right\} \\ &= B(T_c)\, \exp\left\{ \frac{-13 N_g\, C}{T_c^5} \int_0^{q(T)} \frac{q\, \gamma(q)}{(1-q^2)^{7/2}}\, dq \right\}, \end{aligned} \tag{6.10}$$

with $q(T) = \sqrt{1 - T^2/T_c^2}$. This is our final result; it describes how the erasure of the BAU, measured by $B_0/B_{T_c}$, can be obtained by an integration of $\gamma(T)$ over the temperature. In the next two sections we present numerical results of this ratio from which we deduce an upper bound on the Higgs mass.

# 7 Numerical Results

In this section we present the results of our numerical calculations. We take $m_W = 83$ GeV, $g = 0.67$ which is the physical value of the coupling constant and vary the top quark mass in the range 150 to 200 GeV, i.e. around its recently stated value of 174 GeV [21]. The only unknown physical parameter left is the Higgs mass $m_H$. We discussed the fermion loop contribution already in [17] so in this work we will focus our attention on the evaluation of the bosonic loops.

As we explained, all our results are obtained by a diagonalization of the boson fluctuation matrix $\mathcal{K}_{\rm bos}$ and the Faddeev–Popov matrix $\mathcal{K}_{\rm FP}$ (3.21) in a discretized basis. The spectrum of the matrices must not depend on the choice of the gauge for the classical sphaleron fields. Since we evaluated the matrix for an arbitrary gauge with non-vanishing $C$-field (see eq. (A.25)), it is possible to check the invariance of the spectrum under gauge transformations eq. (3.10). We find that the eigenstates are indeed invariant under gauge transformations if their energy is less than about $0.8\,P_{\rm max}$ where $P_{\rm max}$ is the numerical parameter which restricts the momentum of the eigenstates and renders the basis finite to allow a numerical diagonalization (see eq. (A.11)). Eigenstates with energies close to $P_{\rm max}$ can be gauge dependent which is due to the finite numerical box and should not be encountered in our calculations. Hence we always have to choose $P_{\rm max}$ large enough so that all eigenstates which enter the calculations have energies less than $0.8\,P_{\rm max}$ and, of course, no result changes if $P_{\rm max}$ is further increased.

Another check of the spectrum consists in an investigation of the negative and zero modes. The negative mode appears in the grand-spin $K = 0$ sector of the fluctuation matrix $\mathcal{K}_{\rm bos}$. We checked that its energy is gauge invariant and independent of the box parameters $P_{\rm max}$ and $R$. Moreover our results agree with the ones obtained in [28, 29] where the negative mode has previously been calculated. The zero modes can be identified in the $K = 1$ sector. Due to the spherical symmetry in this sector each state is (2K+1=3)-fold degenerate so that we find two threefold degenerate

states with zero eigenvalue. Numerically the modulus of the eigenvalues was found to be below $10^{-3}$ which shows that the diagonalization reproduces the zero modes with excellent accuracy. The eigenfunctions of the zero modes can be evaluated analytically in terms of the sphaleron background fields [13]. We compared these functions with those which we obtained as zero mode eigenfunctions in the diagonalization and again found a very good agreement.

Beside these investigations of specific eigenstates we checked a property of the spectrum as a whole. For low values of the proper time parameter $t$ we consider the expansion

$$\begin{aligned} \sum_n \left( e^{-t\omega_n^2} - e^{-t(\omega_n^0)^2} \right) &= \mathrm{Tr} \left( \exp[-t\mathcal{K}_{\mathrm{bos}}] - \exp[-t\mathcal{K}_{\mathrm{bos}}^{(0)}] \right) \\ &= a_{\mathrm{bos}} t^{-1/2} + b_{\mathrm{bos}} t^{1/2} + c_{\mathrm{bos}} t^{3/2} + \cdots \end{aligned} \tag{7.1}$$

where the coefficients are given in eqs. (B.4–B.6). Taking $m_H = m_W$, in Fig. 1 we compare the exact result (solid line) for the trace $\mathrm{Tr} \left( \exp[-t\mathcal{K}_{\mathrm{bos}}] - \exp[-t\mathcal{K}_{\mathrm{bos}}^{(0)}] \right)$ (l.h.s. of eq. (7.1)) with several approximations (dashed and dotted lines), given by the first, the first two and all three terms of the r.h.s. of eq. (7.1). For low values of $t$ we obtain excellent agreement between the numerical result and the approximations, as it should be. For large values of $t$ the comparison does not provide a check of the numerical treatment. Here the approximations behave as some power law of $t^{1/2}$ while the exact result is dominated by the contribution of the negative and zero modes, given by $e^{t|\omega_-^2|} + 6$, which is also plotted in Fig. 1 (dashed line).

Now that we have checked the reliability of the spectrum we can use it to calculate the desired quantities. These are the renormalized non-thermal contributions $E^{\mathrm{ren}}_{\mathrm{bos,FP}}$ and the temperature dependent parts $E^{\mathrm{small}}_{\mathrm{bos,FP}}(T)$ associated with the Bose–Einstein distribution factor. Both quantities have to be evaluated for the fluctuation operator $\mathcal{K}_{\mathrm{bos}}$ and the Faddeev–Popov operator $\mathcal{K}_{\mathrm{FP}}$.

To obtain the renormalized value of the non-thermal parts $E^{\mathrm{ren}}_{\mathrm{bos,FP}}$ we have to evaluate $E^{\mathrm{conv}}_{\mathrm{bos,FP}}(\Lambda)$ in the limit of infinite proper time cutoff ($\Lambda \to \infty$) (see eq. (4.11)). Numerically, however, we always have to work with a finite $\Lambda$ to ensure the finiteness of the basis. For this reason the numerical parameters $R$ (box size) and $P_{\max}$ (maximum momentum) also have to be finite. In order to obtain the limit of infinite parameters we proceed as for the fermion non-thermal energy in [17]: First we fix $\Lambda$ and take $R$ and $P_{\max}$ large enough so that their further increasement would not change the result any more. This procedure is repeated with larger values of the cutoff $\Lambda$ until

we can determine the limit $E^{\rm conv}(\Lambda = \infty) = E^{\rm ren}$. We illustrate this method in Tabs. 1 and 2 at the example $m_H = m_W$. The renormalization scale $\nu_{\rm ren}$ is fixed according to eq. (4.25). With $m_t = 174$ we obtain $\nu_{\rm ren} = 2.02$. In Tab. 1 we show results of $E^{\rm conv}_{\rm bos}(\Lambda)$ for fixed $\Lambda = 4$ and various values of $R$ and $P_{\rm max}$. We find that for $R = 12$ and $P_{\rm max} = 16 = 4\,\Lambda$ the continuum limit $E^{\rm conv}_{\rm bos}(\Lambda = 4) = -6.28\,m_W$ is reached with an accuracy of better than 0.2%. With the same method we obtain results for other values of $\Lambda$ which are presented in Tab. 2. For large $\Lambda$ the law $E^{\rm conv}_{\rm bos}(\Lambda) = a + b/\Lambda^2$ is satisfied for the fit $a = -5.95\,m_W$ and $b = -5.7\,m_W$. Thus from the data in Tab. 2 we can extrapolate the result for infinite cutoff $\Lambda$ and obtain $E^{\rm ren}_{\rm bos} = a = -5.95\,m_W$. Considering the possible error of the values for fixed $\Lambda$ and the error of the extrapolation process we estimate an accuracy of better than 2% for the final result. For other Higgs masses the deviations can be slightly bigger but in general the numerical error for the non-thermal energy should be well below 5%.

Table 3 shows results for the renormalized non-thermal energy for different Higgs masses including the contribution from the Faddeev–Popov operator. The renormalization scale $\nu_{\rm ren}$, fixed by eq. (4.25), is included in Tab. 3. As already mentioned in Sect. 4, for $m_H = 350$ GeV eq. (4.25) has no solution so that instead we choose $\nu_{\rm ren}$ to minimize the difference between $m_H$ and the pole Higgs mass, which for this reason may deviate from 350 GeV by some value less than 10%. Moreover we give values for the classical sphaleron energy and for the fermion non-thermal energy. The latter was calculated for $\frac{3}{2}$ heavy doublets with top quark masses between 150 and 200 GeV and $9 + \frac{3}{2}$ massless doublets. We find that both the fermion and the boson non-thermal energy are significantly lower than the classical energy which is in accordance with the fact that, generally speaking, loop contributions are suppressed by a factor $\alpha$ relative to the tree contribution. Actually after the renormalization the non-thermal energy of the boson fluctuations about the sphaleron is small and negative while that of the fermions is larger and positive. However, we show below that the thermal part dominates the boson fluctuations and the sum of both parts has the same sign as the classical energy.

The behavior of the non-thermal energies for low $m_H$ and large $m_t$ can be described by simple scaling laws. For $m_t/m_W > 1$ the aggregate energy density of the Dirac sea is dominated by the square loop diagram in the external Higgs field and hence is proportional to $N_c(h\Phi)^4 \ln(h\Phi/\nu_{\rm ren})$ where $h$ is the Yukawa coupling and $\Phi$ the Higgs field of the sphaleron. To obtain the energy we have to integrate this value over the

space where the Higgs field differs from its vacuum expectation value, i.e. over the spread of the sphaleron. For small Higgs masses $m_H/m_W \ll 1$ the size of the sphaleron fields roughly scales as $m_H^{-1}$ since the asymtotic behavior for large radial distance $r$ is dominated by the term $e^{-(m_H/m_W)\,r}$. Therefore all spatial integrals and hence all matrix elements of the fluctuation matrices scale as $m_H^{-3}$. Thus for $m_H < m_W < m_t$ the dependence of the zero temperature energies on $m_t$ and $m_H$ is roughly given by

$$E^{\rm ren}_{\rm ferm} \;\propto\; +N_c\,\frac{m_t^4\,\ln(m_t/\nu_{\rm ren}m_W)}{m_H^3}\,, \tag{7.2}$$

$$E^{\rm ren}_{\rm bos} + E^{\rm ren}_{\rm FP} \;\propto\; -\frac{m_W^4}{m_H^3}\,. \tag{7.3}$$

These scaling laws explain the strong increase of the fluctuations for small $m_H$ and large $m_t$, which is in correspondence to our numerical results. As mentioned above, we also found numerically that the boson and fermion non-thermal energies differ in sign.

One finds a strong increase for small $m_H$ and large $m_t$ also for the thermal parts of the fluctuations, but here both fermionic and bosonic contributions are positive. For not too small temperature $T$ the boson fluctuation energy is dominated by its positive thermal contribution so that the sum of the non-thermal and thermal parts is positive for both the boson and the fermion fluctuation. For small $m_H$ and large $m_t$ these sums are large so that they provide a strong suppression of the sphaleron transition rate. If $m_H$ is small enough, this suppression prevents the erasure of the BAU. Thus, we see that the condition that the BAU should survive sets an upper limit on the Higgs mass.

In order to obtain a quantitative result for this upper bound we still have to evaluate the thermal parts $E^{\rm small}\big|_{qm_W}$ (see eqs. (5.4, 5.5)). To simplify notations we will drop the subscript $qm_W$ in what follows. In principle we could evaluate them by a summation over the whole spectrum; numerically, however, it is preferable to sum only over eigenstates with low or medium energy and to use the expansion

$$\varrho(E) = \varrho_\infty + \varrho_2\,\frac{1}{E^2} + \cdots \tag{7.4}$$

(see eq. (B.1)) for the high energy part of the spectrum. To this end we take a smooth function $F(E)$ with the properties $F(E) = 1$ for $E < E_a - E_b$, $F(E) = 0$ for $E > E_a + E_b$ and $0 < F(E) < 1$ for $E_a - E_b < E < E_a + E_b$. Here $E_a$ and $E_b$ are

fixed numerical energy cutoffs, usually we take $E_b = E_a/2$ so that $E_a$ is left as the only parameter. We calculate the thermal energies as follows:

$$\begin{aligned} E^{\rm small}_{\rm bos,FP}(T) &= \pm\frac{1}{\beta}\Big[{\sum_n}'' F(\omega_n)\,\ln\frac{1-e^{-\beta q m_W \omega_n}}{\beta q m_W} - \sum_n F(\omega_n^0)\,\ln\frac{1-e^{-\beta q m_W \omega_n^0}}{\beta q m_W} \\ &\quad - \varrho_\infty \int_0^\infty dE\, F(E)\,\ln\frac{1-e^{-\beta q m_W E}}{\beta q m_W} \\ &\quad + \varrho_2 \int_0^\infty dE\,\frac{1-F(E)}{E^2}\,\ln\frac{1-e^{-\beta q m_W E}}{\beta q m_W}\Big] \end{aligned} \tag{7.5}$$

The integrals in eq. (7.5) can easily be evaluated numerically, in the sum only states with $\omega_n < E_a + E_b$ appear. Now we have to check that numerically $E^{\rm small}$ is independent of the parameter $E_a$. In Table 4 we show results of $\beta E^{\rm small}_{\rm bos}(T)$ in the high temperature limit (see eq. (B.15)) for $m_H = m_W$ and several values of $E_a$. We also give results for the contributions (the sum and the integrals of eq. (7.5)) separately. We find that in the interval $3 < E_a < 8$ both the sum and the integrals in eq. (7.5) drastically depend on $E_a$ but the result for $\beta E^{\rm small}_{\rm bos}$ varies only by about 2%. For smaller values of $E_a$ the expansion eq. (7.4) is not good any more and for larger values of $E_a$ the numerical accuracy of the spectrum decreases due to contributions of states with very large grand spin $K$. For other Higgs masses the variation of $E^{\rm small}_{\rm bos}(T)$ with $E_a$ can be about 5%. Hence for our calculations we choose $4 \le E_a \le 6$ and obtain $E^{\rm small}(T)$ with an accuracy of usually better than 5%.

We are now going to compare our results to the ones obtained by Carson et. al. [15] and Baacke et. al. [16]. There the expression

$$\ln\kappa = -\beta E^{\rm small}_{\rm bos}(T) - \beta E^{\rm small}_{\rm FP}(T) - 6\ln 2 - \ln|\omega_-| \tag{7.6}$$

was evaluated in the high temperature limit $T \to T_c$. In Fig. 2 we show the results of our work as well as those of [15, 16] as a function of the Higgs mass $m_H$. Our data are between those of [15] and [16], they agree with the ones of [16] up to 10%. Apart from numerical uncertainties one reason for the difference could be the renormalization scheme. We have performed the renormalization at zero temperature strictly, as it is usually done. This corresponds to a subtraction of the first term ($\varrho_\infty$) in the high energy expansion (see eq. (7.4)) which is also the first term of the tadpole expansion [30]. In [16], however, all tadpole graphs except the term linear in $T$ have been removed. The difference is then due to the higher order terms which are small for

high $T$ but numerically not completely negligible. There is a larger deviation from the results of [15], only a qualitative agreement for the low $m_H$ behavior is found.

Since the evaluation of the fluctuation determinants eqs. (3.26–3.28) is a rather involved task one seeks for a good approximation procedure which is easy to handle. Before an exact calculation was performed, Carson and McLerran [13] applied an approximation technique by Diakonov, Petrov, and Yung (DPY) [14] to this problem. Later they calculated the boson fluctuation determinant exactly in the high temperature limit [15] and found that the exact and the approximative result deviate by several orders of magnitude. In this section we revisit the DPY method and explain how it can be used to get the the fluctuation determinants to a reasonable accuracy.

Following [13] we consider here the high temperature limit of the boson fluctuation determinant which can be written as an integral over spectral densities:

$$\ln \chi_{\rm bos} \equiv -\beta_c E_{\rm bos}^{\rm small}(T_c) = -\tfrac{1}{2}\int_0^\infty dE \left(\varrho^{\rm bos}(E) - \varrho_\infty^{\rm bos}\right) \ln(E^2)\,. \tag{7.7}$$

where $\varrho^{\rm bos}(E)$ is the spectral density of the boson operator, with the six zero and one negative mode subtracted. Using the identity

$$\ln \alpha = \int_0^\infty \frac{dt}{t}\left(e^{-t} - e^{-t\alpha}\right) \tag{7.8}$$

we arrive at the proper-time representation:

$$\begin{aligned} \ln \chi_{\rm bos} &= -\tfrac{1}{2}\int_0^\infty dE \left(\varrho^{\rm bos}(E) - \varrho_\infty^{\rm bos}\right) \int_0^\infty \frac{dt}{t}\left(e^{-t} - e^{-tE^2}\right) \\ &= \tfrac{1}{2}\int_0^\infty \frac{dt}{t}\left\{\left(\text{ Tr } \exp[-t\mathcal{K}_{\rm bos}] - 6 - \exp(t|\omega_-|^2) - \text{ Tr } \exp[-t\mathcal{K}_{\rm bos}^{(0)}]\right)\right. \\ &\qquad \left. +7e^{-t} - \frac{\varrho_\infty^{\rm bos}}{2}\sqrt{\frac{\pi}{t}}\right\} \end{aligned} \tag{7.9}$$

where $\varrho_\infty^{\rm bos} = 2a/\sqrt{\pi}$ (see eq. (B.8)).

The idea of the DPY method is as follows [14]. The behavior of the integrand at small $t$ can be established from the semiclassical expansion of the "heat kernel", Tr $\exp(-t\mathcal{K})$, see eqs. (4.7, 7.1) and (B.3). Its behavior at large $t$ is governed by negative and zero modes. Therefore, knowing the behavior of the integrand both at small and large $t$, one can approximate the integral of eq. (7.9) as a sum of small- and large-$t$ contributions, separated by some parameter $t_0$,

$$\ln \chi_{\rm bos} = \int_0^\infty dt\, f(t) \approx \int_0^{t_0} dt\, f_{\rm low}(t) + \int_{t_0}^\infty dt\, f_{\rm high}(t) \equiv \ln \tilde{\chi}_{\rm bos}, \tag{7.10}$$

where the separation parameter should be found from the requirement that the sum of the two terms in this equation is stable in $t_0$. Actually it means that $t_0$ is a point where the small- and large-$t$ approximations to the true integrand cross. If that does not happen the method fails. The more terms one knows from both sides, the better is the accuracy of the method.

Using the heat kernel expansion for Tr $\exp(-t\mathcal{K})$, we find the approximation for small $t$

$$f_{\rm low}(t) = \frac{1}{2}\Big(bt^{-\frac{1}{2}} + ct^{\frac{1}{2}} - (7 + |\omega_-|^2) + \frac{t}{2}(7 - |\omega_-|^4)\Big)\,. \tag{7.11}$$

At large $t$ it behaves as

$$f_{\rm high}(t) = \frac{1}{2}\Big(\frac{7e^{-t}}{t} - at^{-\frac{3}{2}}\Big)\,. \tag{7.12}$$

Knowing the coefficients $a$, $b$, $c$, and $|\omega_-|$, one can estimate the fluctuation determinant, eq. (7.9), using eq. (7.10). The result for three different values of the Higgs mass is presented in Table 5, together with the exact value of $\ln \chi_{\rm bos}$. One observes that the accuracy is at the level of 10 to 15%, but that is a price one has to pay if one wishes to avoid a laborous computation of the exact spectrum.

# 8 The upper bound for the Higgs mass

The main issue of our work is the calculation of the sphaleron transition rate $\gamma = \Gamma/V$ according to the Langer–Affleck formula eqs. (3.11, 5.12) including the classical Boltzmann factor, the fermionic and bosonic one-loop contributions and the Jacobian prefactors. We stress again that our calculation is not based on the high temperature limit but was done for arbitrary values of $T$. Therefore, we can compute the rate for the whole temperature range between zero and the critical temperature $T_c$ and perform the integration over $T$ (see eq. (6.10)) to obtain the ratio $B_0/B_{T_c}$. In Fig. 3 we present the contributions $-\beta q E_{\rm class} + \ln \mathcal{F}$ (classical part), $-\beta E_{\rm FERM}$ (fermion loop), and $-\beta E_{\rm BOS}$ (boson loop) of $\ln \gamma$ (according to eqs. (5.12–5.14)) for $m_H = 66$ GeV and $m_H = 100$ GeV. It is convenient to take the parameter $q = \sqrt{1 - T^2/T_c^2}$ as independent variable rather than the temperature $T$ itself.

Qualitatively both pictures of Fig. 3 show the same behaviour, but we find significant quantitative differences. At low temperatures (large $q$) the main contribution to the classical part is the Boltzmann exponent $-\beta q E_{\rm class}$ which decreases with $q$ roughly linearly. For $T \to T_c$ ($q \to 0$) the Jacobian prefactor $\ln \mathcal{F} \sim 7 \ln q(T) \to -\infty$

dominates the classical part. Hence we find a maximum of the classical contribution to the transition rate at about $q \sim 0.1$. For large and medium $q$ the suppression from the fermion loop contribution can be also rather large (in the case $m_H = 66$ GeV it becomes almost as large as the classical one) but it tends to zero in the high $T$ limit $q \to 0$. The bosonic contribution is generally rather small and almost constant over the plotted range of temperatures. In the high temperature limit it does not disappear but it tends to some finite value. Therefore we see that in this limit which was assumed in previous works [8, 5, 13, 15, 16] the boson one-loop contribution is indeed the most important one while fermions decouple. Adding the loop contributions to the classical part, we obtain the total rate which has the same shape as the classical curve, in particular it also has a maximum. Hence if there was any significant baryon number violation after the electroweak phase transition, it must have happened in a short period around this maximum (remember that in Fig. 3 the logarithm $\ln \gamma$ is plotted while $\gamma$ itself enters the integral of eq. (6.10)). We find that the piece of the curve for the total rate which is marked by a solid line contributes about 99% to the ratio $\log_{10}(B_0/B_{T_c})$ which measures the washout of the BAU.

Both the position of this washout area and the value of the maximum are strongly influenced by the loop corrections, especially we note that in this region the fermionic contribution which was neglected in previous works is quite essential. Below we investigate the effect of the fermions quantitatively by computing the ratio $B_0/B_{T_c}$ with and without fermion loop corrections and confirm the significance of the fermions.

Comparing the two plots of Fig. 3, we find that the loop contributions are strong for low $m_H$ so that in this case the rate is suppressed, while for large $m_H$ the fluctuations are rather weak. This is also documented in Fig. 4, where we have plotted the total transition rate for various $m_H$ and $m_t$. In accordance to the scaling laws eqs. (7.2, 7.3) we find a strong suppression of the transition rate $\gamma$ for small $m_H$ and large $m_t$ and a weak suppression for large $m_H$. This results finally for physically relevant $m_t$ in a small transition rate for small $m_H$ and a large transition rate for large $m_H$. If the maximum value of $\gamma$ is small enough, the baryon number violating processes have happened so rarely that they have not affected the BAU. On the other hand a large transition rate means that the sphaleron transitions must have eliminated the baryon asymmetry. Thus, if we fix $m_t$ we obtain an upper bound for $m_H$ below which the asymmetry is conserved and above which we expect a dissipation of the baryon number. This is how we deduce our upper bound from the condition that

the BAU should survive the age of sphaleron transitions.

Before we evaluate this conclusion quantitatively a comment on the limits of the approach is in order. Our calculation is based on the assumption that the Langer–Affleck formula is valid and our restriction to one-loop contributions is justified, i.e. that higher order corrections can be neglected. Both assumptions are reasonable for temperatures not too close to $T_c$ and if the fluctuations on the one-loop level are small compared to the classical part. The physics of the phase transition and in its direct vicinity, where perturbation expansion breaks down, is complicated and not well understood yet so it is difficult to decide at what temperature the framework of our calculation becomes inapplicable and what in this case could be a more adequate description. However, we can estimate the reliability of our model by checking if, first, in the washout region the loop contributions are not too big compared to the classical part, and second, if the onset of the sphaleron transitions, i.e. the left margin of the interval marked by a solid line in the corresponding curve of Fig. 4, is not too close to the critical temperature. Figs. 3 and 4 show that both conditions are well fulfilled for $m_H \gtrsim 100$ GeV but not so good for smaller $m_H$; for $m_H \lesssim 60$ GeV the fluctuations are rather large so that the model on the one-loop level is probably not reliable. The conclusion of this restriction on the applicability of our technical framework will be drawn later.

Furthermore, we assume that, before the transitions start, there is the same number of baryons and leptons in the Universe, i.e. $B - L = 0$. In the standard model $B - L$ is strictly conserved so that this condition will not change during the period of the transitions. If there were a primordial excess of e.g. antileptons, created by unknown forces which violate $B-L$ before the electroweak phase transition, then the sphaleron transitions would increase rather than decrease the BAU.

Let us also briefly comment on the connection between our critical temperature $T_c$ defined in eq. (5.9) and the electroweak phase transition. As a consequence of the thermal renormalization the vacuum expectation value of $\Phi$ becomes $T$ dependent and vanishes for $T \to T_c$. This looks like the behavior of fields at a second order phase transition. However, in order to obtain the true temperature and nature of the phase transition, one would have to include other terms, e.g. a term of the order of $T\Phi^3$ into the potential. Since there is no consistent way how to perform calculations near the phase transition, where perturbation theory is not applicable, we decided to take only the numerically by far dominating term of the order $T^2\Phi^2$ explicitely into

the potential; other terms, like the $T\Phi^3$ one, are considered in the quantum correction $E^{\rm small}$. Thus our critical temperature should be seen as a mere definition which needs not necessarily coincide with the temperature of the true transition, neither do we imply that the phase transition is of second order.

Knowing the transition rate $\gamma$ as a function of $q$ for a fixed Higgs mass $m_H$ it is now possible to perform the integration in eq. (6.10) numerically. The result for the ratio $\log_{10}(B_0/B_{T_c})$ is plotted in Fig. 5 for $m_t$ =150, 174, and 200 GeV. For comparison, we also performed the calculation without considering fermions. In this case we did not use eq. (4.25) to fix the renormalization scale, but a corresponding equation which follows from the Higgs propagator with boson fluctuations included instead of fermions. Here we obtain $\nu_{\rm ren} \sim 1$.

All the curves start at zero for small Higgs masses which means that the BAU survives completely. If we increase $m_H$, the fluctuations become weaker so that the transition rate increases. Hence the ratio $B_0/B_{T_c}$ suddenly begins to fall, and within a short interval it drops by 20 orders of magnitude. The bigger the top quark mass is, the larger are the fluctuations, and hence the region where this decrease takes place is shifted to larger Higgs masses. For a Higgs mass beyond this region the survival of the BAU is ruled out, irrespectively of its initial value $B_{T_c}$ immediately after the phase transition. Let us assume that this initial value is such that in order to explain the present day BAU we have to demand $B_0/B_{T_c} \gtrsim 10^{-5}$ [5] (we see, however, from Fig. 5 that this value is not important since a change by many orders of magnitude alters the upper bound by only a few GeV). For $m_t = 150$ GeV we obtain $m_H \lesssim 60$ GeV, for $m_t = 174$ GeV the upper bound is at 65 GeV, and for $m_t = 200$ GeV the BAU survives if $m_H \lesssim 71$ GeV. At any rate, for all physical choices of the parameters $m_t$ and $B_0/B_{T_c}$ the upper bound for the Higgs mass is found in the range between 60 to 75 GeV.

The calculation without fermions leads to a qualitatively similar picture, but the erasure of the asymmetry happens already at much lower Higgs masses. Assuming $B_0/B_{T_c} \geq 10^{-5}$ we would obtain an upper bound for $m_H$ of only 49 GeV being close to the bound found previously by Bochkarev and Shaposhnikov [6, 5]. The large difference between this value and the bound of 65 GeV which we obtain with fermion fluctuations for $m_t = 174$ GeV again confirms their significance.

# 9 Summary and Conclusions

The present paper investigates the fate of the baryon number asymmetry in the Universe (BAU) after the electroweak phase transition ($T < T_c$). It is assumed that the asymmetry as such originates from baryogenic processes before or during the phase transition with a net result of $B + L \neq 0$ and $B - L = 0$. It is furthermore assumed that in the broken phase ($T < T_c$) the Minimal Standard Model with one Higgs doublet holds. Since the Standard Model does not conserve the baryon number due to possible sphaleron transitions, today's existence of an asymmetry of about $10^{-10}$ baryons per photon implies certain dynamic conditions right after the phase transition which prevent too fast a "wash-out" of the baryon number [7]. In the present paper the baryon number transition rate is evaluated in the one-loop approximation around the classical sphaleron solution (hedgehog). The higher loop effects are partially taken care of by an exact treatment of the "Debye mass" terms, $\sim \Phi^2 T^2$. It is assumed that the Langer–Affleck formula holds and that no baryons are generated in the broken phase.

For all temperatures below the critical temperature $T_c$ the one-loop calculations are performed numerically in the limit of vanishing Weinberg angle. In fact, the baryon number transition rate depends on the classical sphaleron energy, the determinant of the fermionic fluctuations, the determinant of the non-zero bosonic fluctuations, the energy of the negative mode and the normalization factors of the zero modes. While the sphaleron energy and the zero and negative bosonic modes have been calculated previously in the literature [8], the evaluation of non-zero bosonic modes has been performed only in the high temperature limit with somewhat controversial results [15, 16]. In this context the present paper shows the first calculation of the boson determinants for finite temperatures (the fermion determinant at arbitrary temperatures was previously computed by the same authors [17]). It turns out that all above contributions to the transition rate are more or less equally important and must be evaluated at finite temperatures in order to obtain, within the given conceptual frame, an accurate calculation [18].

The actual numbers basically depend only on one unknown parameter, namely the mass of the Higgs boson $m_H$. In fact, the dependence of the baryon number transition rate on the Higgs mass is extremely strong. Both bosonic and fermionic fluctuations above the sphaleron barrier help to preserve the baryon asymmetry in

the Universe. They prevent a fast erasure of the baryon excess provided the mass of the Higgs boson is less than some upper bound, while for larger Higgs masses the sphaleron transition rate becomes large and the asymmetry would be eliminated. The value of this upper bound depends on the mass of the top quark, ranging from about 60 GeV for $m_t = 150$ GeV to 71 GeV for $m_t = 200$ GeV. These results are obtained in the Minimal Standard Model with only one Higgs doublet. They assume a theoretical frame characterized by the applicability of the Langer–Affleck formula and the restriction to one-loop calculations, with a partial resummation of higher orders. These assumptions are only justified if the baryon number violating processes do not happen immediately after the electroweak phase transition where the loop expansion breaks down. This means the position of the maximum of the transition rate $\gamma$ should be not too close to the critical temperature. Moreover the quantum loop contributions at the maximum should be small compared to the classical terms. We find that both conditions are well fulfilled for Higgs masses $m_H \gtrsim 100$ GeV while this is not the case for small Higgs masses below about 60 GeV. Those Higgs masses are, however, ruled out by experiment [31, 32]. Thus we arrive at the following conclusion: If the Higgs mass is in the range between about 60 and 100 GeV, the Minimal Standard Model could be able to account for the survival of the BAU, either within the formal framework we used and a suitable top quark mass or by effects outside this formalism, e.g. higher loop contributions. If it is found above 100 GeV, there is only a little chance to explain the present BAU within the MSM since in this case the application of our framework is rather safe and predicts the complete erasure of the BAU. A possible escape could be an extended model with two Higgs doublets, following from supersymmetric models.

**Acknowledgements:** We are grateful to A.Bochkarev, W.Buchmüller, Z.Fodor, L.McLerran, and M.Shaposhnikov for very useful discussions and comments. We thank P.Pobylitsa for his help on various stages of this work. The work has been sponsored in part by the Deutsche Forschungsgemeinschaft and by the International Science Foundation under Grant No. R2A000. D.D. acknowledges the support of the Alexander von Humboldt Foundation.

# Appendix A

In this appendix we describe how we solve numerically the eigenvalue problems

$$\mathcal{K}_{\rm bos}\Psi_{\rm bos} = \omega^2\Psi_{\rm bos}\,, \qquad\qquad \mathcal{K}_{\rm FP}\Psi_{\rm FP} = \omega^2\Psi_{\rm FP} \tag{A.1}$$

for the boson fluctuation and the Faddeev–Popov operators. We construct a finite basis for the fluctuations in which the operators can numerically be diagonalized. Partially this technique has been developed in the context of the chiral quark model [33, 34, 35] and employed for the diagonalization of the fermionic fluctuation matrix [17], which ensures consistency between the calculations of bosonic and fermionic loop corrections.

The fluctuation vector $\Psi_{\rm bos}$ consists of nine gauge field components $a_i^a$ $(a, i = 1, \ldots, 3)$ and four Higgs field components $\varphi_\mu$ $(\mu = 1, \ldots, 4)$ while $\Psi_{\rm FP}$ contains only three components which we denote by $a_0^a$. Hence the eigenvalue equations read:

$$\begin{pmatrix} \mathcal{G}_{ij}^{ab} & \mathcal{W}_{i\nu}^{a} \\ \mathcal{W}_{j\mu}^{b} & \mathcal{H}_{\mu\nu} \end{pmatrix} \begin{pmatrix} a_j^b \\ \varphi_\nu \end{pmatrix} = \omega^2 \begin{pmatrix} a_i^a \\ \varphi_\mu \end{pmatrix}, \qquad \mathcal{F}^{ab}a_0^b = \omega^2 a_0^a\,, \tag{A.2}$$

where the matrix elements of the fluctuation matrix $\mathcal{K}_{\rm bos}$ are given by (see eq. (3.21))

$$\begin{aligned} \mathcal{G}_{ij}^{ab} &= \delta_{ij}\delta^{ab}\left(-\partial^2 + A_k^c A_k^c + \tfrac{1}{4}\Phi_\mu\Phi_\mu\right) + 2\varepsilon^{abc}F_{ij}^c \\ &\quad + \delta_{ij}\left(\varepsilon^{abc}(\partial_k A_k^c) + 2\varepsilon^{abc}A_k^c\partial_k - A_k^a A_k^b\right), \\ \mathcal{H}_{\mu\nu} &= \delta_{\mu\nu}\left(-\partial^2 + \tfrac{1}{4}A_i^a A_i^a + \tfrac{1}{4}\Phi_\rho\Phi_\rho + \tfrac{1}{8}\nu_H^2(\Phi_\rho\Phi_\rho - 4)\right) \\ &\quad + \eta_{\mu\nu}^a A_i^a\partial_i + \tfrac{1}{2}\eta_{\mu\nu}^a(\partial_i A_i^a) + \tfrac{1}{4}(\nu_H^2 - 1)\Phi_\mu\Phi_\nu\,, \\ \mathcal{W}_{i\nu}^a &= \tfrac{1}{2}\Phi_\nu A_i^a - \tfrac{1}{2}\varepsilon^{abc}\eta_{\mu\nu}^c\Phi_\mu A_i^b - \eta_{\mu\nu}^a(\partial_i\Phi_\mu)\,, \end{aligned} \tag{A.3}$$

and the Faddeev–Popov operator by (see eq. (3.14))

$$\mathcal{F}^{ab} = \delta^{ab}\left(-\partial^2 + A_i^c A_i^c + \tfrac{1}{4}\Phi_\mu\Phi_\mu\right) + \varepsilon^{abc}(\partial_i A_i^c) + 2\varepsilon^{abc}A_i^c\partial_i - A_i^a A_i^b\,. \tag{A.4}$$

For the static classical sphaleron fields we assume the spherically symmetric hedgehog ansatz:

$$\begin{aligned} A_i^a(\mathbf{r}) &= \varepsilon_{aij}n_j\frac{1 - A(r)}{r} + (\delta_{ai} - n_a n_i)\frac{B(r)}{r} + n_a n_i\frac{C(r)}{r}\,, \\ \Phi_i(\mathbf{r}) &= 2\,n_i\,G(r)\,, \qquad \Phi_4(\mathbf{r}) = 2\,H(r)\,. \end{aligned} \tag{A.5}$$

with the given five radial functions $A(r)$, $B(r)$, $C(r)$, $H(r)$, $G(r)$. In principle one of these functions can be eliminated by a gauge transformation. Although this would

lead to a significant simplification of the numerics we will not perform this step but rather stick to the general gauge with five functions since our numerical procedure only works if the classical fields are continuous functions at zero and infinity, i.e. that they take their vacuum values there. This is only possible for a non-vanishing $C$ field, which increases the numerical effort, but on the other hand allows to check the invariance of all quantities under gauge transformations.

To exploit the spherical symmetry and to construct a finite basis in which $\mathcal{K}_{\rm bos}$ and $\mathcal{K}_{\rm FP}$ can numerically be diagonalized we consider a four $(= 3 + 1)$ dimensional reducible $SU(2)$ representation with generators:

$$S_1 = \begin{pmatrix} 0 & 0 & 0 & 0 \\ 0 & 0 & -i & 0 \\ 0 & i & 0 & 0 \\ 0 & 0 & 0 & 0 \end{pmatrix}, \; S_2 = \begin{pmatrix} 0 & 0 & i & 0 \\ 0 & 0 & 0 & 0 \\ -i & 0 & 0 & 0 \\ 0 & 0 & 0 & 0 \end{pmatrix}, \; S_3 = \begin{pmatrix} 0 & -i & 0 & 0 \\ i & 0 & 0 & 0 \\ 0 & 0 & 0 & 0 \\ 0 & 0 & 0 & 0 \end{pmatrix}. \quad \text{(A.6)}$$

A basis of ("spin"-) eigenstates $|S\,S_3\rangle$ of $\mathbf{S}^2 = S_1^2 + S_2^2 + S_3^2$ and $S_3$ is given by

$$|0\,0\rangle = \begin{pmatrix} 0 \\ 0 \\ 0 \\ 1 \end{pmatrix}, \; |1\,1\rangle = \frac{1}{\sqrt{2}} \begin{pmatrix} -i \\ 1 \\ 0 \\ 0 \end{pmatrix}, \; |1\,0\rangle = \begin{pmatrix} 0 \\ 0 \\ i \\ 0 \end{pmatrix}, \; |1\;-1\rangle = \frac{1}{\sqrt{2}} \begin{pmatrix} i \\ 1 \\ 0 \\ 0 \end{pmatrix}. \quad \text{(A.7)}$$

The indices $i, j$ will always refer to coordinates of these spin eigenstates, for example $|1\,1\rangle_{i=1} = -i/\sqrt{2}$, $|0\,0\rangle_{i=4} = 1$. Similarly we define a four dimensional $SU(2)$ "isospin" representation; the operators $T_1$, $T_2$ and $T_3$ and the eigenstates $|T\,T_3\rangle$ look exactly as the corresponding ones of the spin representation. Here the coordinates are referred to by the indices $a, b$ and $\mu, \nu$. Moreover we use the basis $|L\,L_3\rangle$ of the angular momentum operator to describe the spherical space dependence of the fluctuations, with the property

$$\langle \Omega | L\,L_3 \rangle = i^L\, Y_{L\,L_3}(\Omega)\,. \quad \text{(A.8)}$$

The "grand-spin" operator defined by $\mathbf{K} = \mathbf{J} + \mathbf{T} = \mathbf{L} + \mathbf{S} + \mathbf{T}$ commutes with the fluctuation operators of eq. (A.1). Therefore eigenstates of $\mathbf{K}^2$ and $K_3$ form a proper basis for the diagonalization procedure. We couple the eigenstates $|L\,L_3\rangle$, $|S\,S_3\rangle$ and $|T\,T_3\rangle$ to eigenstates of $\mathbf{K}^2$ and $K_3$:

$$|K,\, K_3;\, T,\, J,\, S,\, L\rangle_i^a = \sum_{L_3, S_3, J_3, T_3} C^{K\,K_3}_{J\,J_3,\,T\,T_3}\, C^{J\,J_3}_{L\,L_3,\,S\,S_3}\, |S\,S_3\rangle_i\, |T\,T_3\rangle^a\, |L\,L_3\rangle\,. \quad \text{(A.9)}$$

For the vacuum fluctuation operator, i.e. in the case of no external field, we can solve the eigenvalue problem analytically; the dependence of the fluctuations on the radial coordinate $r$ is in this case given by spherical Bessel functions. We take these solutions as the basis for a numerical diagonalization of $\mathcal{K}$ in the non-vacuum case. To this end we define states $|\, p;\, K,\, K_3;\, T,\, J,\, S,\, L\rangle$ by

$$\langle \mathbf{r} \,|\, p;\, K,\, K_3;\, T,\, J,\, S,\, L\rangle = \mathcal{N}\, j_L(pr)\, \langle \Omega | K,\, K_3;\, T,\, J,\, S,\, L\rangle \,. \tag{A.10}$$

Here the momentum $p$ is a continuous variable, and $\mathcal{N}$ is a normalization factor specified below. In order to get a finite basis we have to discretize the momentum and to restrict its allowed values to a finite number. With large enough numerical box parameters $R$ and $P_{\max}$ we demand:

$$j_I(p_n^I R) = 0\,, \qquad\qquad p_n^I \leq P_{\max} \tag{A.11}$$

where

$$I = I(K,J,S) = \begin{cases} K & \text{for } S=0 \\ J & \text{for } S=1 \end{cases} \,. \tag{A.12}$$

In the case $S = T = 1$ we have three discretization conditions for fixed grand-spin $K$ instead of one, yielding three sets of momenta $p_n^{K+1}$, $p_n^K$, and $p_n^{K-1}$. This extension of the usual construction [34] is necessary to ensure the orthogonality of the basis states; it has already been used and checked in [35]. We obtain

$$\begin{aligned} &\mathcal{N}_n^I \mathcal{N}_m^I \int_0^R dr\, r^2\; j_I(p_n^I r)\, j_I(p_m^I r) \\ &\qquad = \mathcal{N}_n^I \mathcal{N}_m^I \int_0^R dr\, r^2\; j_{I\pm1}(p_n^I r)\, j_{I\pm1}(p_m^I r) = \delta_{nm}\,, \end{aligned} \tag{A.13}$$

if the normalization factor is chosen as

$$\mathcal{N}_n^I = \sqrt{\frac{2}{R^3}}\, \left| j_{I\pm1}(p_n^I R) \right|^{-1} \,; \tag{A.14}$$

hence our states are orthonormal:

$$\begin{aligned} &\langle p_n^I;\, K,\, K_3;\, T,\, J,\, S,\, L \,|\, p_m^{I'};\, K',\, K_3';\, T',\, J',\, S',\, L'\rangle \\ &\qquad = \delta_{nm} \delta_{KK'} \delta_{K_3 K_3'} \delta_{TT'} \delta_{JJ'} \delta_{SS'} \delta_{LL'} \,. \end{aligned} \tag{A.15}$$

For fixed values of $K = 0, 1, 2, \ldots$ and $K_3 = -K, \ldots, +K$ we can write down the following set of basis states for the fluctuations:

$$\Psi_{\text{bos}}^{1,\alpha}(\mathbf{r}) \;=\; \begin{pmatrix} a_i^a(\mathbf{r}) \\ \varphi_a(\mathbf{r}) \\ \varphi_4(\mathbf{r}) \end{pmatrix} = \begin{pmatrix} \langle \mathbf{r} \,|\, p_n^J;\, K,\, K_3;\, 1,\, J,\, 1,\, L\rangle_i^a \\ 0 \\ 0 \end{pmatrix} = \begin{pmatrix} \langle \mathbf{r} \,|\, \widetilde{\Psi}_{\text{bos}}^{1,\alpha}\rangle_i^a \\ 0 \\ 0 \end{pmatrix}$$

$$\text{for } J = K-1, K, K+1;\ L = J-1, J, J+1;\ n = 1, \ldots, N(J);$$

$$\Psi^{2,\alpha}_{\rm bos}(\mathbf{r}) = \begin{pmatrix} a^a_i(\mathbf{r}) \\ \varphi_a(\mathbf{r}) \\ \varphi_4(\mathbf{r}) \end{pmatrix} = \begin{pmatrix} 0 \\ \langle \mathbf{r} \,|\, p^K_n;\ K,\ K_3;\ 1,\ L,\ 0,\ L \rangle^a_4 \\ 0 \end{pmatrix} = \begin{pmatrix} 0 \\ \langle \mathbf{r} \,|\widetilde{\Psi}^{2,\alpha}_{\rm bos} \rangle^a_4 \\ 0 \end{pmatrix}$$
$$\text{for} \quad L = K-1, K, K+1; \quad n = 1, \ldots, N(K);$$

$$\Psi^{3,\alpha}_{\rm bos}(\mathbf{r}) = \begin{pmatrix} a^a_i(\mathbf{r}) \\ \varphi_a(\mathbf{r}) \\ \varphi_4(\mathbf{r}) \end{pmatrix} = \begin{pmatrix} 0 \\ 0 \\ \langle \mathbf{r} \,|\, p^K_n;\ K,\ K_3;\ 0,\ K,\ 0,\ K \rangle^4_4 \end{pmatrix} = \begin{pmatrix} 0 \\ 0 \\ \langle \mathbf{r} \,|\widetilde{\Psi}^{3,\alpha}_{\rm bos} \rangle^4_4 \end{pmatrix}$$
$$\text{for} \quad n = 1, \ldots, N(K);$$

$$\Psi^{\alpha}_{\rm FP}(\mathbf{r}) = a^a_0(\mathbf{r}) = \langle \mathbf{r} \,|\, p^K_n;\ K,\ K_3;\ 1,\ L,\ 0,\ L \rangle^a_4 = \langle \mathbf{r} \,|\widetilde{\Psi}^{\alpha}_{\rm FP} \rangle^a_4$$
$$\text{for} \quad L = K-1, K, K+1; \quad n = 1, \ldots, N(K); \tag{A.16}$$

where $N(I)$ is the number of allowed momenta $p^I_n$, see eq. (A.11). The index $\alpha$ enumerates the basis states of the three groups for the fluctuations and of the Faddeev–Popov matrix. For $K = 0, 1$ not all of these basis states exist. The total number of states for $\Psi_{\rm bos}$ is given by $3N(K+1) + 7N(K) + 3N(K-1)$ for fixed $K > 1$ and fixed $K_3$, for $K = 1$ it is $3N(2) + 7N(1) + N(0)$ and $3N(1) + 2N(0)$ for $K = 0$. For the Faddeev–Popov matrix we have $3N(K)$ basis vectors for $K > 0$ and $N(0)$ for $K = 0$.

We show below that due to the spherical symmetry of the sphaleron the operator $\mathcal{K}_{\rm bos}$ is block diagonal in $K$ and $K_3$, i.e. basis states with different $K$ or $K_3$ do not mix. Moreover the blocks for different $K_3$ and the same $K$ are identical, so that for each $K$ only one matrix has to be diagonalized, and the resulting eigenvalues are $(2K+1)$–fold degenerate. The dimension of this matrix is given by the number of the above basis states. The same holds for the Faddeev–Popov operator $\mathcal{K}_{\rm FP}$.

The remaining task is to calculate the matrix elements of the operators in the basis (A.16); i.e. if $|\, \Psi^{\lambda_1,\,\alpha_1}_{\rm bos} \rangle$ and $|\, \Psi^{\lambda_2,\,\alpha_2}_{\rm bos} \rangle$ are basis states given by eq. (A.16), we need to know the element $\langle \Psi^{\lambda_1,\,\alpha_1}_{\rm bos} | \mathcal{K}_{\rm bos} | \Psi^{\lambda_2,\,\alpha_2}_{\rm bos} \rangle$. For this purpose we have to express the matrices in terms of spherical tensor operators so that the spherical part of the matrix elements can be evaluated analytically. Apart from $\mathbf{S}$ and $\mathbf{T}$ given in eq. (A.6) we

need operators $\mathbf{P}^+$ and $\mathbf{P}^-$, acting in spin space, which we define as

$$P_1^+ = \begin{pmatrix} 0 & 0 & 0 & 1 \\ 0 & 0 & 0 & 0 \\ 0 & 0 & 0 & 0 \\ 1 & 0 & 0 & 0 \end{pmatrix},\ P_2^+ = \begin{pmatrix} 0 & 0 & 0 & 0 \\ 0 & 0 & 0 & 1 \\ 0 & 0 & 0 & 0 \\ 0 & 1 & 0 & 0 \end{pmatrix},\ P_3^+ = \begin{pmatrix} 0 & 0 & 0 & 0 \\ 0 & 0 & 0 & 0 \\ 0 & 0 & 0 & 1 \\ 0 & 0 & 1 & 0 \end{pmatrix}, \tag{A.17}$$

and

$$P_1^- = \begin{pmatrix} 0 & 0 & 0 & -i \\ 0 & 0 & 0 & 0 \\ 0 & 0 & 0 & 0 \\ i & 0 & 0 & 0 \end{pmatrix},\ P_2^- = \begin{pmatrix} 0 & 0 & 0 & 0 \\ 0 & 0 & 0 & -i \\ 0 & 0 & 0 & 0 \\ 0 & i & 0 & 0 \end{pmatrix},\ P_3^- = \begin{pmatrix} 0 & 0 & 0 & 0 \\ 0 & 0 & 0 & 0 \\ 0 & 0 & 0 & -i \\ 0 & 0 & i & 0 \end{pmatrix}. \tag{A.18}$$

It can easily be checked that like $\mathbf{S}$ these operators are spherical vector operators, i.e. $[K_i\,, P_j^\pm] = i\,\varepsilon_{ijk} P_k^\pm$. Moreover we define two scalar operators by

$$I_S = \begin{pmatrix} 1 & 0 & 0 & 0 \\ 0 & 1 & 0 & 0 \\ 0 & 0 & 1 & 0 \\ 0 & 0 & 0 & 0 \end{pmatrix}, \qquad i_S = \begin{pmatrix} 0 & 0 & 0 & 0 \\ 0 & 0 & 0 & 0 \\ 0 & 0 & 0 & 0 \\ 0 & 0 & 0 & 1 \end{pmatrix}. \tag{A.19}$$

In the isospin space we need the corresponding operators which we denote by $\mathbf{Q}^\pm$ and $I_T$, $i_T$.

Using the relations

$$\begin{aligned}
\delta_{ij} &= (I_S)_{ij}\,, \quad \delta^{ab} = (I_T)^{ab}\,, \quad \delta_{\mu\nu} = (I_T + i_T)_{\mu\nu}\,, \\
\varepsilon_{ijk} &= i\,(S_k)_{ij}\,, \quad \varepsilon^{abc} = i\,(T_c)^{ab}\,, \quad \eta^a_{\mu\nu} = i\,(T_a + Q^-_a)_{\mu\nu}\,, \\
A^a_k A^b_k &= (A^c_k A^c_k I_T - A^c_k A^d_k T_d T_c)^{ab}\,, \quad \mathcal{W}^a_{rb} = (\mathcal{W}^k_{rk} I_T - \mathcal{W}^k_{rl} T_l T_k)^{ab}\,, \\
\Phi_\mu \Phi_\nu &= (\Phi_k \Phi_k I_T + \Phi_4 \Phi_4 i_T - \Phi_l \Phi_k T_l T_k + \Phi_k \Phi_4 Q^+_k)_{\mu\nu}\,, \\
(P^+_r)_{i4} &= (P^+_r)_{4i} = (iP^-_r)_{i4} = -(iP^-_r)_{4i} = \delta_{ri}\,, \\
(Q^+_k)^{a4} &= (Q^+_k)^{4a} = (iQ^-_k)^{a4} = -(iQ^-_k)^{4a} = \delta^{ka}
\end{aligned} \tag{A.20}$$

we can rewrite the fluctuation matrices:

$$\begin{aligned}
\mathcal{G}^{ab}_{ij} &= \Big\{ I_T I_S(-\partial^2 + \tfrac{1}{4}\Phi_\mu \Phi_\mu) + I_S T_c T_d A^c_k A^d_k \\
&\qquad + i\,T_c\,(2 I_S A^c_k \partial_k + I_S(\partial_k A^c_k) + i\,\varepsilon_{klm} F^c_{kl} S_m) \Big\}^{ab}_{ij}\,,
\end{aligned}$$

$$
\begin{aligned}
\mathcal{H}_{\mu\nu} &= \Big\{ i_S(I_T + i_T)\,\Big(-\partial^2 + \tfrac{1}{4}A_i^a A_i^a + \tfrac{1}{4}\Phi_\rho\Phi_\rho + \tfrac{1}{8}\nu_H^2(\Phi_\rho\Phi_\rho - 4)\Big) \\
&\quad + i_S(T_a + Q_a^-)\, i\,\Big(A_i^a\partial_i + \tfrac{1}{2}(\partial_i A_i^a)\Big) \\
&\quad + i_S\,\tfrac{1}{4}(\nu_H^2 - 1)\,\Big(\Phi_k\Phi_k I_T + \Phi_4\Phi_4 i_T - \Phi_l\Phi_k T_l T_k + \Phi_k\Phi_4 Q_k^+\Big)\Big\}_{44}^{\mu\nu}, \\
\mathcal{W}_{i\nu}^a &= \Big\{ \tfrac{1}{2}\Big(\mathcal{W}_{rk}^k I_T - \mathcal{W}_{rl}^k T_l T_k\Big)\,(P_r^+ + iP_r^-) \\
&\quad + \tfrac{1}{4}\,\mathcal{W}_{r4}^k\,(Q_k^+ + iQ_k^-)\,(P_r^+ + iP_r^-)\Big\}_{i4}^{a\nu}, \\
\mathcal{W}_{j\mu}^b &= \Big\{ \tfrac{1}{2}\Big(\mathcal{W}_{rk}^k I_T - \mathcal{W}_{rl}^k T_k T_l\Big)\,(P_r^+ - iP_r^-) \\
&\quad + \tfrac{1}{4}\,\mathcal{W}_{r4}^k\,(Q_k^+ - iQ_k^-)\,(P_r^+ - iP_r^-)\Big\}_{4j}^{\mu b}, \\
\mathcal{F}^{ab} &= \Big\{ i_S I_T(-\partial^2 + \tfrac{1}{4}\Phi_\mu\Phi_\mu) + i_S T_c T_d A_i^c A_i^d \\
&\quad + i_S T_c\, i\,(2A_i^c\partial_i + (\partial_i A_i^c))\Big\}_{44}^{ab}.
\end{aligned}
\tag{A.21}
$$

Now we can find matrices $\widetilde{\mathcal{K}}_{\rm bos}$ and $\widetilde{\mathcal{K}}_{\rm FP}$ with the property

$$
\begin{aligned}
\langle\Psi_{\rm bos}^{\lambda_1,\,\alpha_1}|\,\mathcal{K}_{\rm bos}\,|\Psi_{\rm bos}^{\lambda_2,\,\alpha_2}\rangle &= \langle\widetilde{\Psi}_{\rm bos}^{\lambda_1,\,\alpha_1}|\,\widetilde{\mathcal{K}}_{\rm bos}\,|\widetilde{\Psi}_{\rm bos}^{\lambda_2,\,\alpha_2}\rangle\,, \\
\langle\Psi_{\rm FP}^{\alpha_1}|\,\mathcal{K}_{\rm FP}\,|\Psi_{\rm FP}^{\alpha_2}\rangle &= \langle\widetilde{\Psi}_{\rm FP}^{\alpha_1}|\,\widetilde{\mathcal{K}}_{\rm FP}\,|\widetilde{\Psi}_{\rm FP}^{\alpha_2}\rangle
\end{aligned}
\tag{A.22}
$$

(for the definition of the states $|\,\widetilde{\Psi}_{\rm bos}^{\lambda,\,\alpha}\rangle$ and $|\,\widetilde{\Psi}_{\rm FP}^{\alpha}\rangle$ see eq. (A.16)):

$$
\begin{aligned}
\widetilde{\mathcal{K}}_{\rm bos} &= I_T I_S(-\partial^2 + \tfrac{1}{4}\Phi_\mu\Phi_\mu) + I_S T_c T_d A_k^c A_k^d + I_S T_c\Big(2A_k^c\, i\,\partial_k + i\,(\partial_k A_k^c)\Big) \\
&\quad - \varepsilon_{klm}F_{kl}^c S_m T_c + i_S(I_T + i_T)\,\Big(-\partial^2 + \tfrac{1}{4}A_i^a A_i^a\Big) \\
&\quad + i_S I_T\Big(\Big(\tfrac{1}{4} + \tfrac{1}{8}\nu_H^2\Big)\,\Phi_4\Phi_4 + \tfrac{3}{8}\nu_H^2\Phi_k\Phi_k - \tfrac{1}{2}\nu_H^2\Big) \\
&\quad + i_S i_T\Big(\Big(\tfrac{1}{4} + \tfrac{1}{8}\nu_H^2\Big)\,\Phi_k\Phi_k + \tfrac{3}{8}\nu_H^2\Phi_4\Phi_4 - \tfrac{1}{2}\nu_H^2\Big) \\
&\quad + i_S(T_a + Q_a^-)\,\Big(A_i^a\, i\,\partial_i + \tfrac{1}{2}(i\,\partial_i A_i^a)\Big) \\
&\quad + \tfrac{1}{4}(\nu_H^2 - 1)\,\Big(i_S Q_k^+\Phi_k\Phi_4 - i_S T_l T_k\Phi_k\Phi_l\Big) + I_T P_r^+\mathcal{W}_{rk}^k \\
&\quad - \tfrac{1}{2}\varepsilon_{klm}\mathcal{W}_{rl}^k T_m P_r^- - \tfrac{1}{2}\,\Big(\mathcal{W}_{rl}^k + \mathcal{W}_{rk}^l\Big)\,T_l T_k P_r^+ \\
&\quad + \tfrac{1}{2}\mathcal{W}_{r4}^k\,\Big(Q_k^+ P_r^+ - Q_k^- P_r^-\Big)\,, \\
\widetilde{\mathcal{K}}_{\rm FP} &= i_S I_T(-\partial^2 + \tfrac{1}{4}\Phi_\mu\Phi_\mu) + i_S T_c T_d A_i^c A_i^d + i_S T_c\Big(2A_i^c\, i\,\partial_i + i\,(\partial_i A_k^c)\Big)\,.
\end{aligned}
\tag{A.23}
$$

Our next step is to plug in the hedgehog ansatz (A.5) so that the matrices $\widetilde{\mathcal{K}}_{\rm bos}$ and $\widetilde{\mathcal{K}}_{\rm FP}$ can be expressed through the profile functions $A$, $B$, $C$, $H$, $G$, and the spherical

vector and scalar operators. With the hedgehog ansatz and

$$\partial_i = n_i \, \tfrac{\partial}{\partial r} - \tfrac{i}{r} \, \varepsilon_{ijk} n_j L_k \tag{A.24}$$

we obtain after a long and tedious calculation:

$$\begin{aligned}
\widetilde{\mathcal{K}}_{\rm bos} \;=\; & \Big(-\tfrac{\partial^2}{\partial r^2} - \tfrac{2}{r}\,\tfrac{\partial}{\partial r} + \tfrac{\mathbf{L}^2}{r^2} + G^2 + H^2 + \tfrac{2}{r^2}\Big((1-A)^2 + B^2\Big)\Big) I_T I_S \\
& + \tfrac{1}{r^2}\Big(C^2 - B^2 - (1-A)^2\Big) I_S \, (\mathbf{n}\cdot\mathbf{T})^2 + \tfrac{2}{r^2}\,(1-A)\, I_S \, (\mathbf{T}\cdot\mathbf{L}) \\
& + \tfrac{i}{r^2}\Big(2rC\tfrac{\partial}{\partial r} + rC' + C\Big) I_S \, (\mathbf{n}\cdot\mathbf{T}) + \tfrac{2B}{r^2}\, I_S \Big(\mathbf{T}\cdot(\mathbf{n}\times\mathbf{L}) - i\,(\mathbf{n}\cdot\mathbf{T})\Big) \\
& + \tfrac{2}{r^2}\Big(1 - A^2 - B^2 + rA' + BC\Big)\,(\mathbf{n}\cdot\mathbf{S})\,(\mathbf{n}\cdot\mathbf{T}) \\
& + \tfrac{2}{r^2}\,(rB' - AC)\,\mathbf{n}\cdot(\mathbf{S}\times\mathbf{T}) - \tfrac{2}{r^2}\,(rA' + BC)\,(\mathbf{S}\cdot\mathbf{T}) \\
& + \Big(-\tfrac{\partial^2}{\partial r^2} - \tfrac{2}{r}\,\tfrac{\partial}{\partial r} + \tfrac{\mathbf{L}^2}{r^2} + \tfrac{1}{2r^2}\Big((1-A)^2 + B^2 + \tfrac{C^2}{2}\Big)\Big) i_S (I_T + i_T) \\
& + \Big(H^2 + \tfrac{1}{2}\nu_H^2 (H^2 - 1) + \tfrac{3}{2}\nu_H^2 G^2\Big) i_S I_T \\
& + \Big(G^2 + \tfrac{1}{2}\nu_H^2 (G^2 - 1) + \tfrac{3}{2}\nu_H^2 H^2\Big) i_S i_T + (1 - \nu_H^2)\, G^2 \, i_S \, (\mathbf{n}\cdot\mathbf{T})^2 \\
& \tfrac{1}{r^2}\,(1-A)\, i_S \, (\mathbf{T} + \mathbf{Q}^-)\cdot\mathbf{L} + \tfrac{i}{2r^2}\Big(2rC\tfrac{\partial}{\partial r} + rC' + C\Big)\, i_S \, \mathbf{n}\cdot(\mathbf{T} + \mathbf{Q}^-) \\
& + \tfrac{B}{r^2}\, i_S \Big((\mathbf{T} + \mathbf{Q}^-)\cdot(\mathbf{n}\times\mathbf{L}) - i\,\mathbf{n}\cdot(\mathbf{T} + \mathbf{Q}^-)\Big) \\
& - (1 - \nu_H^2)\, HG \, i_S \, (\mathbf{n}\cdot\mathbf{Q}^+) + \tfrac{1}{r}\,\left(GC + 2rH'\right)\, I_T \, (\mathbf{n}\cdot\mathbf{P}^+) \\
& - \tfrac{1}{r}\,(G + GA - HB)\,(\mathbf{T}\cdot\mathbf{P}^-) + \tfrac{1}{r}\,(H - HA - BG)\,\mathbf{n}\cdot(\mathbf{T}\times\mathbf{P}^-) \\
& + \tfrac{1}{r}\,(G + GA - HB + HC - 2rG')\,(\mathbf{n}\cdot\mathbf{T})\,(\mathbf{n}\cdot\mathbf{P}^-) \\
& + \tfrac{1}{2r}\,(H - HA - BG)\,\mathbf{n}\cdot(\mathbf{Q}^+\times\mathbf{P}^+ - \mathbf{Q}^-\times\mathbf{P}^-) \\
& - \tfrac{1}{2r}\,(G + GA - HB)\,(\mathbf{Q}^+\cdot\mathbf{P}^+ - \mathbf{Q}^-\cdot\mathbf{P}^-) \\
& + \tfrac{1}{2r}\,(G + GA - HB + HC - 2rG') \\
& \qquad\qquad \Big((\mathbf{n}\cdot\mathbf{Q}^+)\,(\mathbf{n}\cdot\mathbf{P}^+) - (\mathbf{n}\cdot\mathbf{Q}^-)\,(\mathbf{n}\cdot\mathbf{P}^-)\Big)\,, \\
\widetilde{\mathcal{K}}_{\rm FP} \;=\; & \Big(-\tfrac{\partial^2}{\partial r^2} - \tfrac{2}{r}\,\tfrac{\partial}{\partial r} + \tfrac{\mathbf{L}^2}{r^2} + G^2 + H^2 + \tfrac{2}{r^2}\Big((1-A)^2 + B^2\Big)\Big) i_S I_T \\
& + \tfrac{1}{r^2}\Big(C^2 - B^2 - (1-A)^2\Big)\, i_S \, (\mathbf{n}\cdot\mathbf{T})^2 + \tfrac{2}{r^2}\,(1-A)\, i_S \, (\mathbf{T}\cdot\mathbf{L}) \\
& + \tfrac{i}{r^2}\Big(2rC\tfrac{\partial}{\partial r} + rC' + C\Big)\, i_S \, (\mathbf{n}\cdot\mathbf{T}) + \tfrac{2B}{r^2}\, i_S \Big(\mathbf{T}\cdot(\mathbf{n}\times\mathbf{L}) - i\,(\mathbf{n}\cdot\mathbf{T})\Big)\,,
\end{aligned} \tag{A.25}$$

where we dropped the argument $r$ of the profile functions. Now it is easy to see that all the spherical operators which turn up in eq. (A.25) are scalar operators in the

sense that they commute with the grand-spin $\mathbf{K}^2$ and $K_3$ so that

$$\left[\widetilde{\mathcal{K}}_{\rm bos}\,,\,\mathbf{K}^2\right]=\left[\widetilde{\mathcal{K}}_{\rm bos}\,,\,K_3\right]=0\,,\qquad\left[\widetilde{\mathcal{K}}_{\rm FP}\,,\,\mathbf{K}^2\right]=\left[\widetilde{\mathcal{K}}_{\rm FP}\,,\,K_3\right]=0\,. \tag{A.26}$$

This is the reason why the matrices can be diagonalized in each $K$ sector separately, as mentioned above.

For the numerical diagonalization one has to evaluate these matrices in the basis (A.16). The radial part of a matrix element leads to a numerical computation of a one dimensional integral. The angular part, however, can be evaluated analytically. The most direct and easiest way to do this is to employ the Wigner–Eckart theorem and perform the summations over the Clebsch–Gordan coefficients with the help of a program like *Mathematica*. Instead of writing down the complete result of this angular integration we demonstrate the procedure with an example. We consider the operator $\frac{1}{r}\,(GC+2rH')\,I_T\,(\mathbf{n}\cdot\mathbf{P}^+)$ which is part of $\widetilde{\mathcal{K}}_{\rm bos}$ and calculate the matrix element

$$\begin{aligned}&\Big\langle p_n^J;\,K,K_3;\,1,\,J,\,1,\,L\,\Big|\,\tfrac{1}{r}\,(GC+2rH')\,I_T\,(\mathbf{n}\cdot\mathbf{P}^+)\,\Big|\,p_m^K;\,K,K_3;\,1,\,L',\,0,\,L'\Big\rangle\\&\quad=\mathcal{N}_n^J\mathcal{N}_m^K\int_0^R dr\;r^2\,j_L(p_n^Jr)\,\tfrac{1}{r}\,(GC+2rH')\,j_{L'}(p_m^K)\\&\qquad\cdot\Big\langle\,K,K_3;\,1,\,J,\,1,\,L\,\Big|\,I_T\,(\mathbf{n}\cdot\mathbf{P}^+)\,\Big|\,K,K_3;\,1,\,L',\,0,\,L'\,\Big\rangle\,.\end{aligned} \tag{A.27}$$

The integral over the radial coordinate $r$ has to be evaluated numerically. The angular matrix element is independent of $K_3$ so that we can put $K_3$ to zero. We obtain:

$$\begin{aligned}&\Big\langle\,K,0;\,1,\,J,\,1,\,L\,\Big|\,I_T\,(\mathbf{n}\cdot\mathbf{P}^+)\,\Big|\,K,0;\,1,\,L',\,0,\,L'\,\Big\rangle\\&\quad=\sum_{L_3,S_3,J_3,T_3}\;\sum_{L_3',T_3'}\;\sum_{m=-1}^{1}(-1)^m\,C^{K\,0}_{J\,J_3,\,1\,T_3}\,C^{J\,J_3}_{L\,L_3,\,1\,S_3}\,C^{K\,0}_{L'\,L_3',\,1\,T_3'}\\&\qquad\cdot\langle\,1\,T_3\,|\,I_T\,|\,1\,T_3'\,\rangle\,\langle\,1\,S_3\,|\,P^+_{(m)}\,|\,0\,0\,\rangle\,\langle\,L\,L_3\,|\,n_{(-m)}\,|\,L'\,L_3'\,\rangle\,.\end{aligned} \tag{A.28}$$

Here the operators $P^+_{(m)}$ and $n_{(-m)}$ are spherical, not cartesian components of $\mathbf{P}^+$ and $\mathbf{n}$. The matrix elements in the last line can subsequently be evaluated using the Wigner–Eckart theorem, e.g.

$$\langle\,1\,S_3\,|\,P^+_{(m)}\,|\,0\,0\,\rangle=\frac{1}{\sqrt{3}}\,C^{1\,S_3}_{0\,0,\,1\,m}\,\langle\,1\,||\,\mathbf{P}^+\,||\,0\,\rangle\,. \tag{A.29}$$

Hence for the calculation of the matrix element in eq. (A.27) we need to perform a numerical integration, a summation over Clebsch–Gordan coefficients, and to know

the following reduced matrix elements:

$$\begin{aligned}
\langle\, L \,||\, \mathbf{L} \,||\, L' \,\rangle &= \delta_{LL'}\, \sqrt{L(L+1)(2L+1)}\,, \\
\langle\, L \,||\, \mathbf{n} \,||\, L' \,\rangle &= \delta_{|L-L'|,\,1}\, (-i)\, \sqrt{\tfrac{1}{2}(L+L'+1)}\,, \\
\langle\, L \,||\, \mathbf{n}\times\mathbf{L} \,||\, L' \,\rangle &= \begin{cases} -(L-1)\sqrt{L} & \text{for } L' = L-1 \\ (L+2)\sqrt{L+1} & \text{for } L' = L+1 \\ 0 & \text{otherwise} \end{cases}\,, \\
\langle\, S \,||\, \mathbf{S} \,||\, S' \,\rangle &= \delta_{SS'}\, \sqrt{S(S+1)(2S+1)}\,, \\
\langle\, S \,||\, I_S \,||\, S' \,\rangle &= \sqrt{3}\,\delta_{S1}\,\delta_{S'1}\,, \\
\langle\, S \,||\, i_S \,||\, S' \,\rangle &= \delta_{S0}\,\delta_{S'0}\,, \\
\langle\, S \,||\, \mathbf{P}^+ \,||\, S' \,\rangle &= -i\,\sqrt{3}\,(\delta_{S1}\,\delta_{S'0} + \delta_{S0}\,\delta_{S'1})\,, \\
\langle\, S \,||\, \mathbf{P}^- \,||\, S' \,\rangle &= -\sqrt{3}\,(\delta_{S1}\,\delta_{S'0} - \delta_{S0}\,\delta_{S'1})\,.
\end{aligned} \tag{A.30}$$

For the correspoding reduced matrix elements of the isospin states one simply has to replace $S$ by $T$ and $P$ by $Q$.

# Appendix B

We discuss here the spectral densities $\varrho(E)$ defined in eq. (5.1), especially their asymptotic behavior for large $E$. It is easy to see that at large $E$ one can expand the spectral density in a series

$$\varrho(E) \sim \varrho_\infty + \sum_{n=1}^{\infty} \varrho_{2n} E^{-2n}\,. \tag{B.1}$$

In order to calculate the values of the coefficients

$$\lim_{E\to\infty} \varrho(E) = \varrho_\infty \qquad \text{and} \qquad \lim_{E\to\infty} \Big(\varrho(E) - \varrho_\infty\Big) E^2 = \varrho_2 \tag{B.2}$$

we use the small $t$ expansion of

$$\begin{aligned}
F(t) &= \mathrm{Tr}\,\Big(\exp[-t\mathcal{K}] - \exp[-t\mathcal{K}^{(0)}]\Big) = \sum_{\substack{\text{discrete}\\ \text{levels}}} e^{-t\omega^2} + \int_0^\infty dE\,\varrho(E)\,e^{-tE^2} \\
&= a t^{-1/2} + b t^{1/2} + c t^{3/2} + \cdots\,.
\end{aligned} \tag{B.3}$$

The corresponding coefficients can be easily calculated using gradient expansion, following the renormalization procedure eqs. (4.7–4.10) one can read off

$$a_{\mathrm{FP}} = -\tfrac{3}{32\pi^{3/2}} \int d^3\mathbf{r}\,(\bar\Phi^\dagger\bar\Phi - 4)\,,$$

$$
\begin{aligned}
a_{\rm bos} &= -\tfrac{3}{32\pi^{3/2}}(4+\nu_H^2)\int d^3\mathbf{r}\,(\bar\Phi^\dagger\bar\Phi-4)\,, \\
a_{\rm ferm} &= -\tfrac{1}{8\pi^{3/2}}\,N_c\nu_t^2\int d^3\mathbf{r}\,(\bar\Phi^\dagger\bar\Phi-4) \qquad\qquad (B.4)\\
b_{\rm FP} &= \tfrac{1}{16\pi^{3/2}}\int d^3\mathbf{r}\,\Big(-\tfrac{1}{3}(\bar F_{ij}^a)^2+\tfrac{3}{16}(\bar\Phi^\dagger\bar\Phi-4)^2+\tfrac{3}{2}(\bar\Phi^\dagger\bar\Phi-4)\Big)\,, \\
b_{\rm bos} &= \tfrac{1}{16\pi^{3/2}}\int d^3\mathbf{r}\,\Big(\tfrac{41}{6}(\bar F_{ij}^a)^2+\tfrac{3}{16}(4-3\nu_H^2+\nu_H^4)(\bar\Phi^\dagger\bar\Phi-4)^2\,, \\
&\qquad\qquad +\tfrac{3}{4}(8-3\nu_H^2+\nu_H^4)(\bar\Phi^\dagger\bar\Phi-4)\Big)\,, \\
b_{\rm ferm} &= \tfrac{1}{16\pi^{3/2}}\int d^3\mathbf{r}\,\Big(\tfrac{1}{3}\,N_g(N_c+1)(\bar F_{ij}^a)^2+\tfrac{1}{8}\,N_c\nu_t^2(2\nu_t^2-\nu_H^2)(\bar\Phi^\dagger\bar\Phi-4)^2\,, \\
&\qquad\qquad +\tfrac{1}{2}\,N_c\nu_t^2(4\nu_t^2-\nu_H^2)(\bar\Phi^\dagger\bar\Phi-4)\Big)\,, \qquad\qquad (B.5)
\end{aligned}
$$

where we made use of eq. (3.8) to eliminate the term $(\bar D_i\bar\Phi)^\dagger(\bar D_i\bar\Phi)$ in $b_{\rm bos}$ and $b_{\rm ferm}$. In Section 7 we also need [13]

$$
\begin{aligned}
c_{\rm bos} &= -\tfrac{1}{384\pi^{3/2}}\int d^3\mathbf{r}\,\Big[2\nu_H^2\bar F_{ij}^a\bar F_{ij}^a+\tfrac{28}{15}\,\varepsilon^{abc}\bar F_{ij}^a\bar F_{jk}^b\bar F_{ki}^c \\
&\qquad +\tfrac{1}{4}\,(-3\nu_H^2+93)\,(\bar\Phi^\dagger\bar\Phi)\,\bar F_{ij}^a\bar F_{ij}^a+\tfrac{1}{8}\,(5\nu_H^4-4\nu_H^2+\tfrac{449}{5})\,[\partial_i(\bar\Phi^\dagger\bar\Phi)]^2 \\
&\qquad +\tfrac{1}{2}\,(\nu_H^4+28\nu_H^2+\tfrac{31}{5})\,(\bar\Phi^\dagger\bar\Phi)\,(\bar D_i\bar\Phi)^\dagger(\bar D_i\bar\Phi) \\
&\qquad +\tfrac{1}{32}\,(15\nu_H^6+21\nu_H^4+18\nu_H^2+48)\,(\bar\Phi^\dagger\bar\Phi-4)^3 \\
&\qquad +\tfrac{1}{8}\,(27\nu_H^6+57\nu_H^4+36\nu_H^2+144)\,(\bar\Phi^\dagger\bar\Phi-4)^2 \\
&\qquad +9\,(\nu_H^6+2\nu_H^4+\nu_H^2+8)\,(\bar\Phi^\dagger\bar\Phi-4)\Big]\,. \qquad\qquad (B.6)
\end{aligned}
$$

Using (B.3) one can show that

$$
\lim_{t\to0}\sqrt{t}\,F(t)=\tfrac{1}{2}\,\sqrt{\pi}\,\varrho_\infty\,, \qquad\qquad (B.7)
$$

which implies

$$
\varrho_\infty=2a/\sqrt{\pi}\,. \qquad\qquad (B.8)
$$

To calculate $\varrho_2$, let us introduce the function $R(E)$ such that

$$
R'(E)=\varrho(E)\quad\text{and}\quad R(0)=n_D=\text{number of discrete levels}\,, \qquad\qquad (B.9)
$$

$n_D^{\rm FP}=0\,,\ n_D^{\rm bos}=7\,,\ n_D^{\rm ferm}=1\,.$ Using partial integration, we can write

$$
\begin{aligned}
&\frac{\sqrt{t}\,F(t)-a}{t}=\frac{1}{\sqrt{t}}\Big(\sum_{\substack{\text{discrete}\\ \text{levels}}}e^{-t\omega^2}+\int_0^\infty dE\,\Big(\varrho(E)-\varrho_\infty\Big)\,e^{-tE^2}\Big) \\
&=\frac{1}{\sqrt{t}}\Big(\sum_{\substack{\text{discrete}\\ \text{levels}}}e^{-t\omega^2}+\Big(R(E)-\varrho_\infty E\Big)\,e^{-tE^2}\Big|_0^\infty\Big)+2\sqrt{t}\int_0^\infty dE\,\Big(R(E)-\varrho_\infty E\Big)\,E\,e^{-tE^2} \\
&=\frac{1}{\sqrt{t}}\sum_{\substack{\text{discrete}\\ \text{levels}}}(e^{-t\omega^2}-1)+2\sqrt{t}\int_0^\infty dE\,\Big(R(E)-\varrho_\infty E\Big)\,E\,e^{-tE^2}\,. \qquad\qquad (B.10)
\end{aligned}
$$

The first term vanishes with $t \to 0$, and for the second one we can use the same way as above with $\Big(R(E) - \varrho_\infty E\Big)\, E$ instead of $\varrho(E)$ and find that

$$\lim_{E\to\infty} \Big(R(E) - \varrho_\infty E\Big)\, E = \frac{b}{\sqrt{\pi}} \,. \tag{B.11}$$

Using l'Hospital's rule we finally find

$$\varrho_2 = \lim_{E\to\infty} \Big(\varrho(E) - \varrho_\infty\Big)\, E^2 = -\frac{b}{\sqrt{\pi}} \,. \tag{B.12}$$

From eq. (B.11) we can deduce another interesting result; $\lim\limits_{E\to\infty} \Big(R(E) - \varrho_\infty E\Big) = 0$ yields

$$\int_0^\infty dE \, \Big(\varrho(E) - \varrho_\infty\Big) = \lim_{E\to\infty} \Big(R(E) - \varrho_\infty E - R(0)\Big) = -R(0) = -n_{_D} \,. \tag{B.13}$$

Finally we show that the contributions $E^{\rm small}_{\cdots}$ to the transition rate $\gamma$ are finite in the high temperature limit, i.e. $q \to 0$. In the fermionic case we obtain by partial integration

$$\begin{aligned} E^{\rm small}_{\rm ferm}\Big|_{qm_W} &= -\tfrac{1}{\beta} \int_0^\infty dE \, \Big(\varrho^{\rm ferm}(E) - \varrho^{\rm ferm}_\infty\Big) \, \ln(1 + e^{-\beta q m_W E}) - \tfrac{1}{\beta}\, n^{\rm ferm}_{_D} \ln 2 \\ &= \tfrac{1}{\beta} \Big(\underbrace{R^{\rm ferm}(0) - n^{\rm ferm}_{_D}}_{0}\Big) \ln 2 - q m_W \int_0^\infty dE \, \frac{R^{\rm ferm}(E) - \varrho^{\rm ferm}_\infty E}{1 + e^{\beta q m_W E}} \\ &\stackrel{q\to 0}{\longrightarrow} \; 0 \,. \end{aligned} \tag{B.14}$$

For $E^{\rm small}_{\rm bos}$ and $E^{\rm small}_{\rm FP}$ we obtain

$$\begin{aligned} E^{\rm small}_{\cdots}\Big|_{qm_W} &= \pm\tfrac{1}{\beta} \int_0^\infty dE \, \Big(\varrho^{\cdots}(E) - \varrho^{\cdots}_\infty\Big) \, \ln \frac{1 - e^{-\beta q m_W E}}{\beta q m_W} \\ &\stackrel{q\to 0}{\longrightarrow} \; \pm\tfrac{1}{\beta} \int_0^\infty dE \, \Big(\varrho^{\cdots}(E) - \varrho^{\cdots}_\infty\Big) \, \ln E \qquad \text{(finite)} \end{aligned} \tag{B.15}$$

The last line holds since this is true for the integral $\int_0^E$ with arbitrary upper bound $E$, and the rest $\int_E^\infty$ vanishes with growing $E$ due to the behavior of $\varrho(E) - \varrho_\infty$, eq. (B.12).

# References


[1] A.D.Dolgov and Ya.B.Zeldovich, *Rev. Mod. Phys.* **53**, 1 (1981);
A.G.Cohen, D.B.Kaplan, and A.E.Nelson, *Ann. Rev. Nucl. Part. Sci.* **43**, (1993).

[2] G.'t Hooft, *Phys. Rev. Lett.* **37**, 8 (1976).

[3] L.D.Faddeev, in *Proceedings of the IVth International Conference on Nonlocal Field Theories*, Dubna, USSR, 1976 (Joint Institute for Nuclear Research, Dubna, 1976).

[4] R.Jackiw and C.Rebbi, *Phys. Rev. Lett.* **37**, 172 (1976).

[5] A.Bochkarev and M.Shaposhnikov, *Mod. Phys. Lett.* **A2**, 417 (1987).

[6] M.Shaposhnikov, *Nucl. Phys.* **B287**, 757 (1987); **B299**, 797 (1988).

[7] V.Kuzmin, V.Rubakov, and M.Shaposhnikov, *Phys. Lett.* **B155**, 36 (1985); **B191**, 171 (1987).

[8] P.Arnold and L.McLerran, *Phys. Rev.* **D36**, 581 (1987); **37**, 1020 (1988).

[9] J.Langer, *Ann. Phys. (N.Y.)* **41**, 108 (1967); **54**, 258 (1969).

[10] I.Affleck, *Phys. Rev. Lett.* **46**, 388 (1981).

[11] R.Dashen, B.Hasslacher, and A.Neveu, *Phys. Rev.* **D10**, 4138 (1974).

[12] N.Manton, *Phys. Rev.*, **D28**, 2019 (1983);
F.R.Klinkhamer and N.S.Manton, *Phys. Rev.* **D30**, 2212 (1984).

[13] L.Carson and L.McLerran, *Phys. Rev.* **D41**, 647 (1990).

[14] D.Diakonov, V.Petrov, and A.Yung, *Sov. J. Nucl. Phys.* **39**, 150 (1984);
D.Diakonov, V.Petrov, and A.Yung, *Phys. Lett.* **130B**, 240 (1984).

[15] L.Carson, X.Li, L.McLerran, and R.-T.Wang, *Phys. Rev.* **D42**, 2127 (1990).

[16] J.Baacke and S.Junker, *Phys. Rev.* **D49**, 2055 (1994);
Erratum, *Phys. Rev.* **D50**, 4227 (1994).

[17] D.Diakonov, M.Polyakov, P.Sieber, J.Schaldach, and K.Goeke, *Phys. Rev.* **D49**, 6864 (1994).

[18] D.Diakonov, M.Polyakov, P.Pobylitsa, P.Sieber, J.Schaldach,
and K.Goeke, *Phys. Lett.* **B336**, 457 (1994).

[19] A.Bochkarev, *Phys. Lett.* **B254**, 165 (1991).

[20] T.Gould and I.Rothstein, *Phys. Rev.* **D48**, 5917 (1993).

[21] F.Abe et al., *Phys. Rev. Lett.* **73**, 225 (1994); Preprint FERMILAB-PUB-95-022-E, 1995; S.Abachi et al., Preprint FERMILAB-PUB-95-028-E, 1995.

[22] J.Kunz, B.Kleihaus, and Y.Brihaye, *Phys. Rev.* **D46**, 3587 (1992).

[23] D.A.Kirzhnitz and A.D.Linde, *Ann. Phys.* **101**, 195 (1976).

[24] A.N.Redlich and L.C.R.Wijewardhana, *Phys. Rev. Lett.* **54** 970 (1985).

[25] D.Diakonov and V.Petrov, *Phys. Lett.* **275B**, 459 (1992).

[26] S.Weinberg, *Gravitation and Cosmology*, John Wiley & Sons, 1972.

[27] K.Olive, in *Proceedings of the 33rd International Winter School on Nuclear and Particle Physics*, Schladming, Austria, 1994 (Springer Verlag, Berlin, 1994).

[28] T.Akiba, H.Kikuchi, and T.Yanagida, *Phys. Rev.* **D40**, 588 (1989).

[29] Y.Brihaye, S.Giler, P.Kosinski, and J.Kunz, *Phys. Rev.* **D42**, 2846 (1990).

[30] L.Dolan and R.Jackiw, *Phys. Rev.* **D9**, 3320 (1979).

[31] T.R.Wyatt, *The status of searches for the standard model Higgs boson at LEP*, Preprint CERN-PPE/94-71 (1994).

[32] A.Sopczak, *Status of Higgs hunting at LEP — Five Years of Progress* , Preprint CERN-PPE/95-46 (1995).

[33] S.Kahana and G.Ripka, *Nucl. Phys.* **A429**, 962 (1984);
G.Ripka and S.Kahana, *Phys. Rev.* **D36**, 1233 (1987).

[34] Th.Meissner, F.Grümmer, and K.Goeke, *Phys. Lett.* **B306**, 296 (1989);
Th.Meissner, E.Ruiz Arriola, and K.Goeke, *Z. Phys.* **A336**, 91 (1990);
K.Goeke et. al., *Phys. Lett.* **B256**, 321 (1991).

[35] P.Sieber, M.Praszalowicz, and K.Goeke, *Nucl. Phys.* **A569**, 629 (1994);
Z.Dulinski, M.Praszalowicz, and P.Sieber, *Acta Phys. Pol.* **B24**, 1931 (1993).

| $R$ | 10 | 10 | 10 | 12 | 14 |
|---|---|---|---|---|---|
| $P_{\max}$ | 12 | 14 | 16 | 16 | 16 |
| $E_{\rm bos}^{\rm conv}(\Lambda = 4)/m_W$ | $-6.25$ | $-6.29$ | $-6.29$ | $-6.28$ | $-6.28$ |

**Tab. 1:** $E_{\rm bos}^{\rm conv}(\Lambda = 4)$ for different values of the numerical parameters $R$ and $P_{\max}$. The result shows that $R = 12$ and $P_{\max} = 16 = 4\,\Lambda$ are large enough to ensure that the continuum limit is reached. The mass parameters are $m_H = m_W = 83$ GeV, $m_t = 174$ GeV, $\nu_{\rm ren} = 2.02$.

| $\Lambda$ | 2 | 3 | 4 | 4.5 | 5 | 5.5 | 6 |
|---|---|---|---|---|---|---|---|
| $E_{\rm bos}^{\rm conv}(\Lambda)/m_W$ | $-6.85$ | $-6.47$ | $-6.28$ | $-6.22$ | $-6.18$ | $-6.14$ | $-6.11$ |

**Tab. 2:** $E_{\rm bos}^{\rm conv}(\Lambda)$ for various values of $\Lambda$. Using the behaviour $E_{\rm bos}^{\rm conv}(\Lambda) = E_{\rm bos}^{\rm ren} + b/\Lambda^2$ for large $\Lambda$, we find by extrapolation the continuum limit $E_{\rm bos}^{\rm ren} = -5.95\, m_W$. The mass parameters are $m_H = m_W = 83$ GeV, $m_t = 174$ GeV, $\nu_{\rm ren} = 2.02$.

| $m_H$ [GeV] | 50 | 66 | 66 | 66 | 83 | 100 | 150 | 350 |
|---|---|---|---|---|---|---|---|---|
| $m_t$ [GeV] | 174 | 150 | 174 | 200 | 174 | 174 | 174 | 174 |
| $\nu_{\rm ren}$ | 2.07 | 1.74 | 2.05 | 2.36 | 2.02 | 1.98 | 1.76 | 2.11 |
| $E_{\rm bos}^{\rm ren}/m_W$ | $-9.74$ | $-5.40$ | $-7.22$ | $-9.32$ | $-5.95$ | $-5.09$ | $-3.64$ | $-5.69$ |
| $E_{\rm FP}^{\rm ren}/m_W$ | 1.36 | 0.48 | 0.75 | 1.10 | 0.46 | 0.29 | 0.08 | $-0.01$ |
| $(E_{\rm bos}^{\rm ren} + E_{\rm FP}^{\rm ren})/m_W$ | $-8.38$ | $-4.92$ | $-6.47$ | $-8.22$ | $-5.49$ | $-4.80$ | $-3.56$ | $-5.69$ |
| $E_{\rm ferm}^{\rm ren}/m_W$ | 26.94 | 10.35 | 16.91 | 26.81 | 12.11 | 9.40 | 5.87 | 4.05 |
| $E_{\rm class}/m_W$ | 96.94 | 99.60 | 99.60 | 99.60 | 101.94 | 104.08 | 109.27 | 121.67 |

**Tab. 3:** The renormalized non-thermal energy of the boson fluctuations $E_{\rm bos}^{\rm ren}$, of the Faddeev–Popov operator $E_{\rm FP}^{\rm ren}$, and the sum of both for various values of the Higgs and the top quark mass. For comparison the classical sphaleron energy $E_{\rm class}$ and the fermionic non-thermal energy $E_{\rm ferm}^{\rm ren}$ are included. The renormalization scale is determined according to eq. (4.25).

| $E_a$ | 2.0 | 3.0 | 4.0 | 6.0 | 8.0 |
|---|---|---|---|---|---|
| $E_b$ | 1.0 | 1.5 | 2.0 | 3.0 | 4.0 |
| 1st line of eq. (7.5) (sum) | 2.54 | 10.95 | 21.93 | 49.95 | 83.95 |
| 2nd and 3rd lines of eq. (7.5) (integrals) | 3.64 | −4.20 | −15.07 | −43.10 | −77.13 |
| $\beta_c E_{\rm bos}^{\rm small}(T_c)$ | 6.18 | 6.74 | 6.85 | 6.85 | 6.82 |

**Tab. 4:** $\beta_c E_{\rm bos}^{\rm small}(T_c)$ and its contributions for several values of the numerical parameters $E_a$ and $E_b$. The contributions strongly depend on $E_a$ and $E_b$, but $E_{\rm bos}^{\rm small}$ is very stable in the range $3 \leq E_a \leq 8$.

| $m_H$ [GeV] | 66 | 83 | 125 |
|---|---|---|---|
| $\ln \chi_{\rm bos}$ | −11.66 | −6.85 | −1.96 |
| $\ln \tilde{\chi}_{\rm bos}$ | −12.91 | −7.66 | −2.27 |

**Tab. 5:** Exact and approximate results for the high temperature limit of the boson fluctuation determinant for various $m_H$. The exact values $\ln \chi_{\rm bos}$ are determined by a summation over the spectrum of eigenvalues of the fluctuation operator, the approximate values $\ln \tilde{\chi}_{\rm bos}$ are obtained with the DPY-method [14]. One finds an accuracy of about 10 to 15%.

This figure "fig1-1.png" is available in "png"  format from:

http://arXiv.org/ps/hep-ph/9502245v2

This figure "fig1-2.png" is available in "png" format from:

http://arXiv.org/ps/hep-ph/9502245v2

This figure "fig1-3.png" is available in "png"  format from:

http://arXiv.org/ps/hep-ph/9502245v2

This figure "fig1-4.png" is available in "png"  format from:

http://arXiv.org/ps/hep-ph/9502245v2

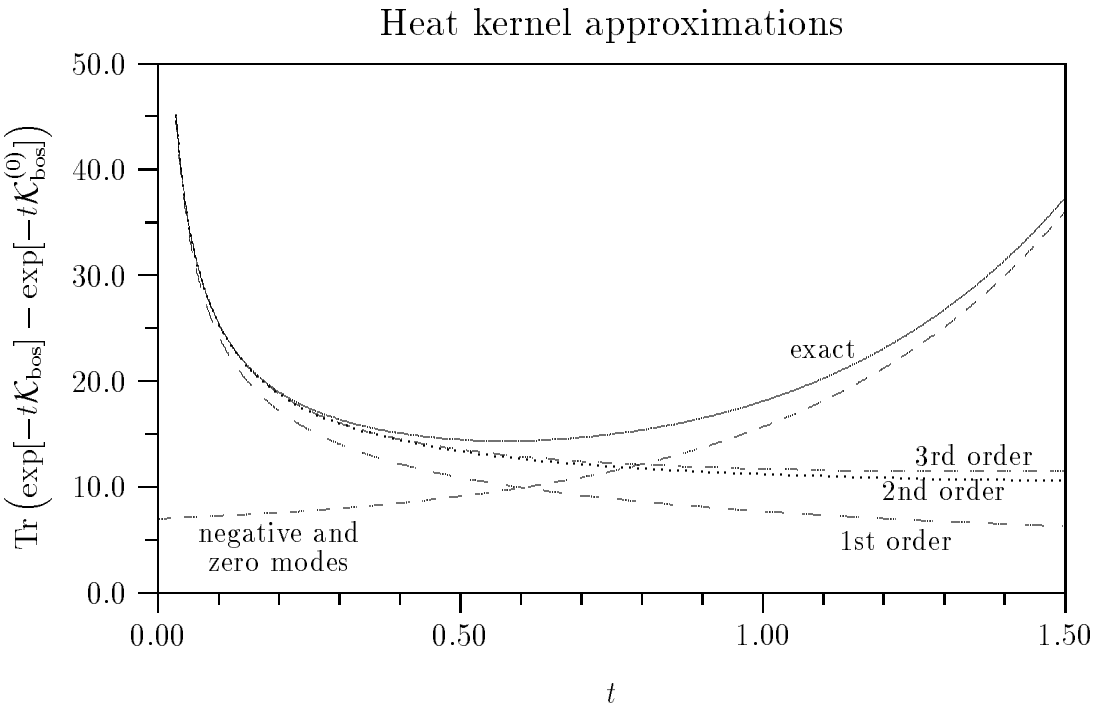


**Fig. 1:** Exact (solid line) and approximate values (dashed and dotted lines) of the heat kernel $\mathrm{Tr}\left(\exp[-t\mathcal{K}_{\mathrm{bos}}] - \exp[-t\mathcal{K}^{(0)}_{\mathrm{bos}}]\right)$ in dependence of the proper time parameter $t$. The exact result is obtained with the discretized spectrum of the fluctuation operator $\mathcal{K}_{\mathrm{bos}}$, the approximations are the first three orders of the expansion in eq. (7.1). For low $t$ we obtain excellent agreement. The large $t$ behaviour of the heat kernel is governed by the negative and zero modes (dashed line).

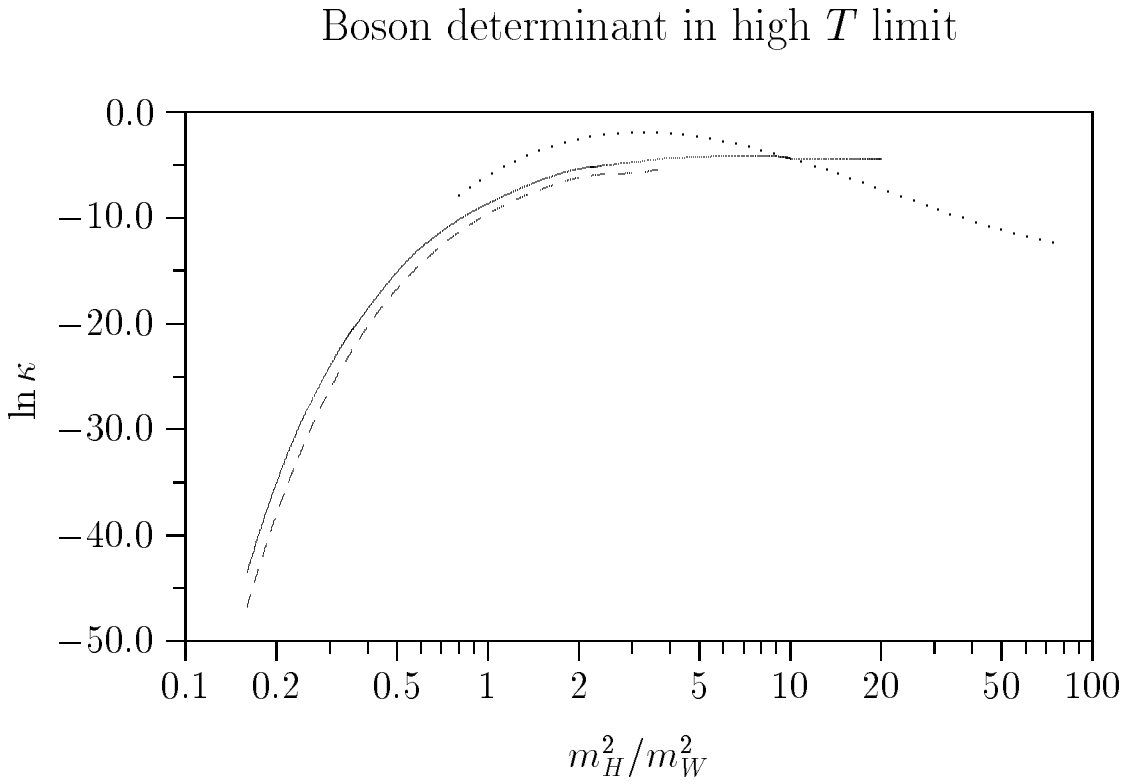


**Fig. 2:** $\ln \kappa = -\beta_c E_{\rm bos}^{\rm small}(T_c) - \beta_c E_{\rm FP}^{\rm small}(T_c) - 6 \ln 2 - \ln |\omega_-|$ as a function of the Higgs mass. We compare our results (solid line) with those of Baacke et. al. [16] (dashed line) and Carson et. al. [15] (dotted line).

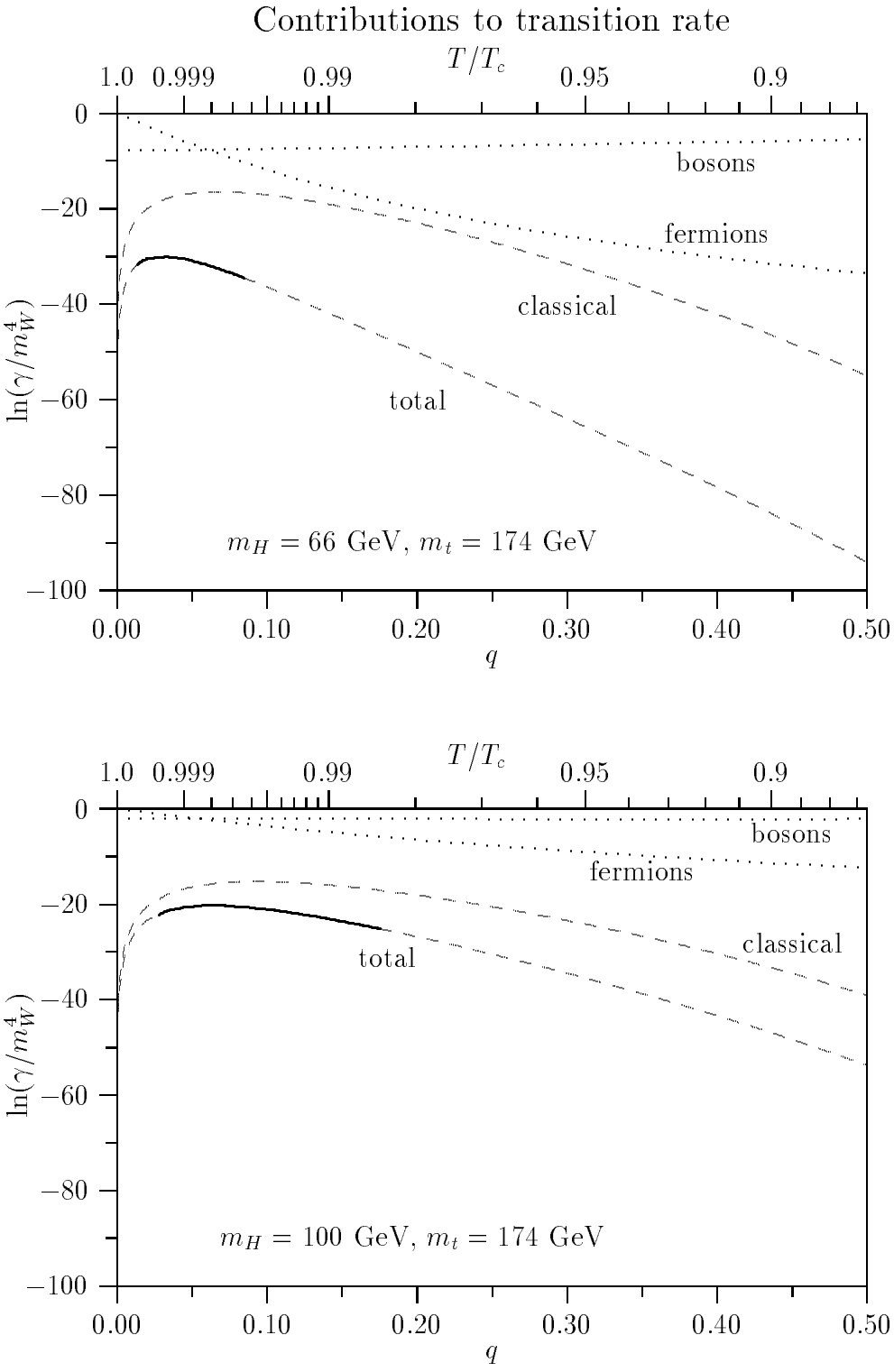


**Fig. 3:** Contributions to the transition rate $\ln\gamma$ for fixed $m_H = 66$ GeV, $m_t = 174$ GeV and $m_H = 100$ GeV, $m_t = 174$ GeV as a function of the parameter $q = \sqrt{1 - T^2/T_c^2}$. The total rate has a maximum close to the critical temperature. The region which mainly contributes to the integral eq. (6.10) is marked by a solid line.

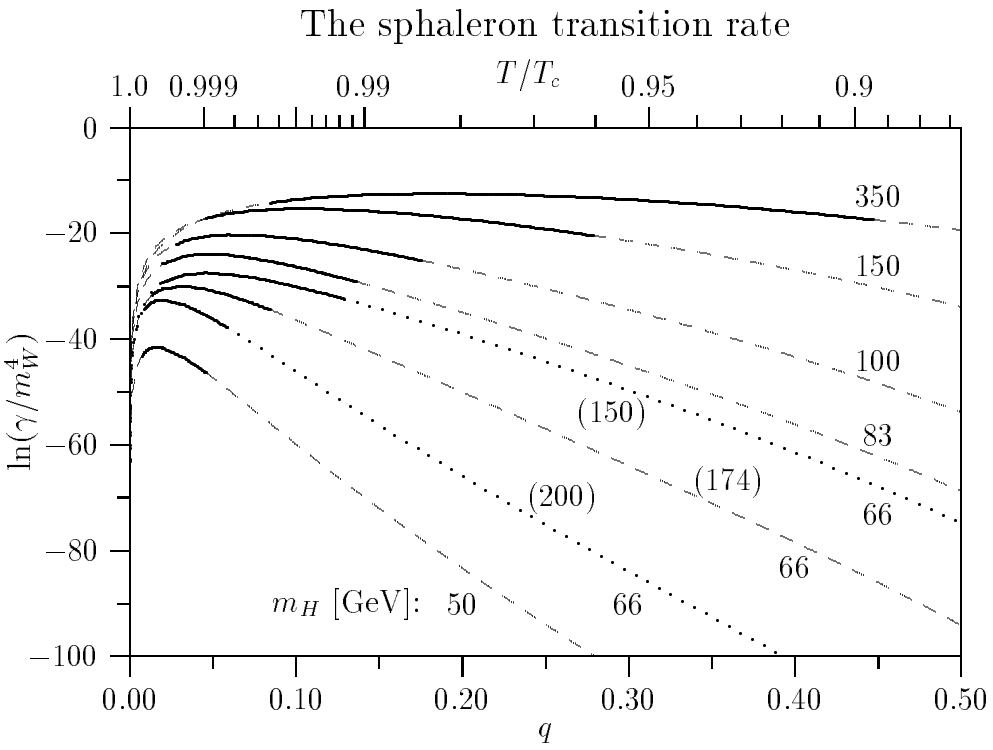


**Fig. 4:** The sphaleron transition rate $\ln(\gamma/m_W^4)$ for various values of $m_H$ (given without brackets) and $m_t$ (given in brackets) depending on the parameter $q = \sqrt{1 - T^2/T_c^2}$. The dashed lines are for $m_t = 174$ GeV, the dotted lines for $m_t = 150$ and 200 GeV. The regions which mainly contribute to the baryon number violation are marked by solid lines.

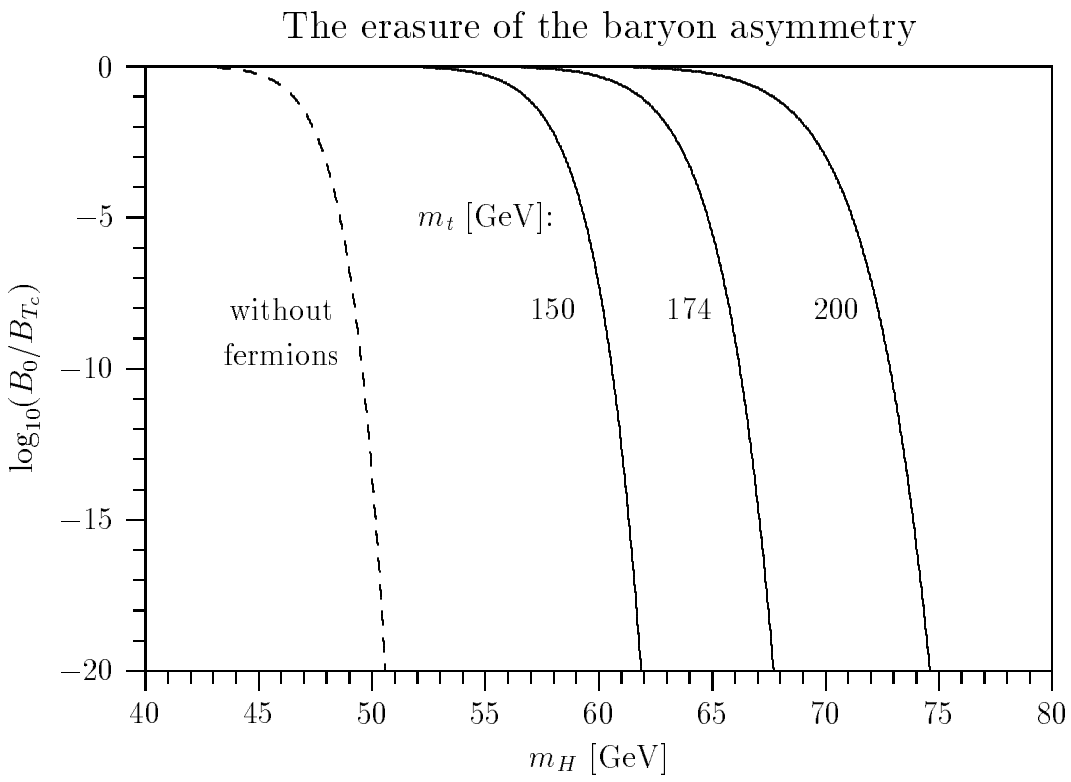


**Fig. 5:** The ratio $B_0/B_{T_c}$ as a function of the Higgs mass $m_H$ for $m_t$ = 150, 174, and 200 GeV. From the condition that this ratio should be at least $10^{-5}$ we obtain an upper bound for $m_H$ in the range 60 to 75 GeV. The same calculation without fermion loops leads to a qualitatively similar picture but the upper bound would be as low as 49 GeV.